Multiplexed, Quantitative Workflow for Sensitive Biomarker Discovery in Plasma Yields Novel Candidates for Early Myocardial Injury*[S]

Hasmik Keshishian‡¶, Michael W. Burgess‡, Michael A. Gillette‡§, Philipp Mertins‡, Karl R. Clauser‡, D. R. Mani‡, Eric W. Kuhn‡, Laurie A. Farrell§, Robert E. Gerszten‡§, and Steven A. Carr‡¶

We have developed a novel plasma protein analysis platform with optimized sample preparation, chromatography, and MS analysis protocols. The workflow, which utilizes chemical isobaric mass tag labeling for relative quantification of plasma proteins, achieves far greater depth of proteome detection and quantification while simultaneously having increased sample throughput than prior methods. We applied the new workflow to a time series of plasma samples from patients undergoing a therapeutic, "planned" myocardial infarction for hypertrophic cardiomyopathy, a unique human model in which each person serves as their own biologic control. Over 5300 proteins were confidently identified in our experiments with an average of 4600 proteins identified per sample (with two or more distinct peptides identified per protein) using iTRAQ four-plex labeling. Nearly 3400 proteins were quantified in common across all 16 patient samples. Compared with a previously published label-free approach, the new method quantified almost five-fold more proteins/sample and provided a six- to nine-fold increase in sample analysis throughput. Moreover, this study provides the largest high-confidence plasma proteome dataset available to date. The reliability of relative quantification was also greatly improved relative to the label-free approach, with measured iTRAQ ratios and temporal trends correlating well with results from a 23-plex immunoMRM (iMRM) assay containing a subset of the candidate proteins applied to the same patient samples. The functional importance of improved detection and quantification was reflected in a markedly expanded list of significantly regulated proteins that provided many new candidate biomarker proteins. Preliminary evaluation of plasma sample labeling with TMT six-plex and ten-plex reagents suggests that even further increases in multiplexing of plasma analysis are practically achievable without significant losses in depth of detection relative to iTRAQ four-plex. These results obtained with our novel platform provide clear demonstration of the value of using isobaric mass tag reagents in plasma-based biomarker discovery experiments. ***Molecular & Cellular Proteomics 14: 10.1074/mcp.M114.046813, 2375–2393, 2015.***

The goal of biomarker discovery studies in plasma or other biological matrices is to identify proteins that are truly differential in abundance between a population of cases and suitable controls, or before and after a relevant perturbation. The approach has generally been to use label-free methods to analyze individual samples from each class or condition, often few in number, and to employ a differential cutoff to discriminate real differences from technical artifacts or biological noise. These cutoffs are frequently arbitrarily determined, but may be informed by variables such as the observed CVs of measured peptides and the total number of samples included in the study.

To reconcile the vast dynamic range and complexity of plasma with the hypothesis that disease-specific markers are likely to be of relatively low abundance, plasma samples for biomarker discovery are often extensively processed before liquid chromatography tandem MS (LC-MS/MS)[1] analysis.

From the ‡Broad Institute of MIT and Harvard, 415 Main St., Cambridge, Massachusetts 02142; §Massachusetts General Hospital, 55 Fruit St., Boston, Massachusetts 02114

Received November 24, 2014, and in revised form, February 26, 2015
Published, MCP Papers in Press, DOI 10.1074/mcp.M114.046813
Author contributions: H.K., M.A.G., P.M., E.W.K., R.E.G., and S.A.C. designed research; H.K. and M.W.B. performed research; L.A.F. contributed new reagents or analytic tools; H.K., M.W.B., P.M., K.R.C., and D.M. analyzed data; H.K., M.A.G., K.R.C., R.E.G., and S.A.C. wrote the paper.

[1] The abbreviations used are: LC-MS/MS, Liquid chromatography-mass spectrometry/mass spectrometry; SCX, strong cation exchange; iTRAQ, Isobaric tags for absolute and relative quantitation; TMT, Tandem mass tags; iMRM, Immuno multiple reaction monitoring; RP-HPLC, Reversed phase- high performance liquid chromatography; HOCM, Hypertrophic obstructive cardiomyopathy; PMI, Planned myocardial infaction; UPLC, Ultrahigh pressure liquid chromatography; FDR, False discovery rate; PSM, Peptide spectrum match; Basic RP, high pH reversed phase chromatography; LC-MRM-MS, Liquid chromatography- multiple reaction monitoring – mass spectrometry; MB, Myoglobin; CKB, Creatine kinase B; CKM, Creatine kinase M; FABP, Fatty acid binding protein; TNNT2, Troponin T, cardiac muscle; TNNI3, Troponin I, cardiac muscle; TNNC1, Troponin C, slow skeletal and cardiac muscles; TNNC2, Troponin C, skeletal muscle; ACLP1, Aortic carboxypeptidase 1; FHL1, Four and a half lim domain protein 1; MYL3, Myosin light chain 3; PF4V1, Platelet factor 4 variant.

Typical approaches to improve depth of detection in plasma include immunoaffinity-based depletion of abundant proteins and offline chromatography at the protein or peptide level using approaches based on separation techniques that differ from the final RP-HPLC separation into the mass spectrometer (*e.g.* strong cation exchange chromatography (SCX), size exclusion chromatography, or reversed phase chromatography at basic pH). Increasing the fraction number in plasma discovery experiments has been shown to increase both the total number of peptides/proteins confidently identified and the relative enrichment of low abundance proteins, (1) with accumulating data supporting reversed phase at basic pH as a particularly effective fractionation strategy (1–3). Unfortunately, such intensive processing of individual samples improves depth of coverage at the dual cost of increased pre-analytical variability and decreased throughput. Pre-analytical variability in turn increases the technical CV and hence the minimum difference that can be reliably measured between samples. As an example of the merits and limitations of such a strategy, we have reported previously on plasma-based biomarker discovery for myocardial injury using a label-free workflow consisting of depletion of the most abundant plasma proteins followed by digestion and extensive fractionation of peptides by SCX chromatography prior to LC-MS/MS analysis (4). Detection of up to 900 proteins per sample time point was achieved by fractionation into 80 sub-samples and analyzing each using a 90 min effective gradient (150 min inject-to-inject). Such extensive fractionation markedly constrained the number of samples that could be analyzed, and the attendant pre-analytical variability contributed to the determination that only relatively large fold-changes in abundance ($>5\times$) could be reliably distinguished by this label-free approach.

Though more quantitative and efficient approaches for biomarker discovery in plasma are clearly warranted, surprisingly few plasma studies have attempted to employ contemporary quantitative proteomic methods in deep profiling experiments. Until recently, the use of iTRAQ and similar labeling methods for plasma proteomics had succeeded in quantifying only a few hundred proteins. Somewhat better results are beginning to be reported. A recent interlaboratory study comparing the performance of several high resolution mass spectrometers with respect to detection and iTRAQ quantification identified 1200 to 1700 proteins in plasma in an iTRAQ fourplex format after two rounds of combined IgY14/Supermix (Sigma-Aldrich, St.Louis, MO) immunoaffinity depletion of samples and partitioning of peptides by isoelectric focusing into 30 fractions (5). In a very large-scale study using immunoaffinity depletion of the six most abundant plasma proteins, 8-plex iTRAQ labeling of peptides and LC-MS/MS analysis of 24 SCX peptide fractions, Cole *et al.* identified and quantified a core set of 982 proteins in at least 50 out of 500 plasma samples allowing for protein identification using a single peptide (6). The total aggregate number of proteins quantified using two or more peptides across all 72 iTRAQ experiments in these experiments was ca. 900, whereas the average number of proteins quantified by two or more peptides per iTRAQ experiment was ca. 300 (personal communication with the author).

We reasoned that the combination of optimized plasma processing protocols, improved chromatography and latest-generation MS systems could further enhance biomarker discovery, enabling practical use of iTRAQ and similar labeling approaches such as TMT (7, 8) for plasma proteomics without sacrificing depth of proteome detection. We deployed and tested these process improvements in the context of ongoing discovery and verification of plasma biomarkers of acute myocardial injury, using the planned myocardial infarction model described previously (4).

EXPERIMENTAL PROCEDURES

Patient Sample Collection—Four patients undergoing planned myocardial infarction (PMI) with alcohol ablation for the treatment of hypertrophic obstructive cardiomyopathy (HOCM) were included in this study (4, 9). All protocols for blood collection were approved by the Massachusetts General Hospital Institutional Review Board, and all subjects gave written informed consent.

Peripheral plasma at baseline, as well as 10, 60, and 240 min post-injury for each patient were included in the study.

Sample Preparation for Discovery Proteomics Study in PMI Patient Samples—

Plasma Depletion and Enzymatic Digestion—Four hundred microliters peripheral plasma from four patients collected at baseline and 10, 60, and 240 min postalcohol ablation was immunoaffinity depleted of 14 most abundant proteins followed by the next ~50 moderately abundant proteins using IgY14 LC20 and Supermix LC10 columns (Sigma-Aldrich, St.Louis, MO). Tandem depletion was performed on Agilent 1100 HPLC (Agilent, Santa Clara, CA) system using Dilution, Stripping, and Neutralization buffers provided by the manufacturer and following manufacturer's instructions (Sigma-Aldrich). Flow through of the Supermix column representing depleted plasma was concentrated and buffer exchanged to 50 mM Ammonium Bicarbonate to the original volume (400 μl) using Amicon 3K concentrators (Millipore, Billerica, MA). Protein concentrations of depleted plasma were determined by BCA protein assay (Thermo Fisher Scientific, Waltham, MA).

Four hundred microliters of IgY14/Supermix depleted peripheral plasma per time point and patient was denatured with 6 M Urea, reduced with 20 mM dithiothreitol at 37 °C for 30 min, and alkylated with 50 mM iodoacetamide at room temperature in the dark for 30 min. Urea concentration was diluted to 2 M with 50 mM ammonium bicarbonate prior to Lys-C digestion (Wako, Richmond, VA) at 1:50 (w:w) enzyme to substrate ratio at 30 °C for 2 h with mixing on the shaker at 850 rpm. Urea was further diluted to less than 1 M prior to overnight digestion with trypsin (Promega, Madison, WI) with 1:50 (w:w) enzyme to substrate ratio at 37 °C with shaking at 850 rpm. Digestion was terminated with formic acid to a final concentration of 1%. The digests were desalted using Oasis HLB 1cc (30 mg) reversed phase cartridges (Waters, Milford, MA) with 0.1% Formic acid and 0.1% Formic acid/80% Acetonitrile as buffers A and B, respectively, using a vacuum manifold. Cartridges were conditioned with 3 $\times$ 500 μl buffer B followed by equilibration with 4 $\times$ 500 μl buffer A. After loading the digests at a reduced flow rate, they were washed with 3 $\times$ 750 μl buffer A and eluted with 3 $\times$ 500 μl buffer B. Eluates were frozen and dried by vacuum centrifugation. Digests were reconsti-

tuted in 400 μl of 0.1% formic acid and post-digestion concentrations were determined by BCA. Based on the post-digestion concentration, 80 μg aliquots were prepared, frozen, dried to dryness by vacuum centrifugation and stored at −80 °C.

Spiking in Synthetic Peptide Mixture—Mixture of 97 heavy labeled synthetic peptides was used for spiking into the different time point samples of three out of the four PMI patient samples. Peptide mixture was spiked in at the time of reconstitution of samples for iTRAQ labeling at the ratio of 1:2:5:10 in the four different channels of iTRAQ four-plex. Total amounts spiked into the samples were as follows: baseline - 1 pmol; 10 min - 2 pmol; 1 h - 5 pmol; 4 h - 10 pmol.

iTRAQ Labeling of Plasma Samples—Eighty micrograms dried aliquots of the four time points (baseline, 10, 60 and 240 min post-injury) for each PMI patient were labeled with iTRAQ four-plex reagent following manufacturer's instructions for labeling plasma (AB Sciex, Framingham, MA), which calls for use of two-fold more reagent for plasma than other samples (cell lysates, tissues, etc). In an effort to eliminate bias toward any iTRAQ channel, different iTRAQ channel layout was used for the different time points of the four PMI patient samples. After reconstituting samples in 30 μl 1 M triethylammonium-bicarbonate (TEAB) 100 μl ethanol was added to each sample. Pooled iTRAQ reagent from two vials was added to each sample, mixed and incubated at room temperature for 1 h. Three microliters of each sample was used to check label incorporation by LC-MS/MS prior to quenching the reaction. Once satisfied with labeling efficiency (> 95% label incorporation) the reactions were quenched by adding Tris pH 8 for a final concentration of 100 mM and incubating at room temperature for 15 min. Labeled samples representing four different time points of a PMI patient were mixed together, dried down and desalted using Oasis HLB 1cc (30 mg) reversed phase cartridges as described above. Eluates were frozen, dried to dryness, and stored at −80 °C.

Evaluation of TMT6 and TMT10 Reagents for Labeling Plasma—For the evaluation of TMT six-plex, and TMT ten-plex reagents (Thermo Fisher Scientific) as well as direct comparison with iTRAQ four-plex reagent pooled normal plasma from commercial sources was used (BioreclamationIVT, Baltimore, MD). Plasma was depleted using IgY14/Supermix immunodepletion strategy and digested as described above. Following digestion and desalting, aliquots of 4 × 80 μg, 6 × 53.3 μg, and 10 × 32 μg aliquots were made for iTRAQ four-plex, TMT six-plex, and TMT ten-plex labeling, respectively. Mixture of the same 97 heavy labeled synthetic peptides was spiked in prior to labeling at the following ratios: for iTRAQ four-plex at 10:5:1:2 ratios corresponding to 114:115:116:117 channels, for TMT six-plex at 10:5:1:1:2:0.5 corresponding to 126:127:128:129:130:131 channels, and for TMT ten-plex at 10:5:0.5:2:1:1:2:3:5:0.5 corresponding to 126:127N:127C:128N:128C:129N:129C:130N:130C:131 channels. iTRAQ labeling of plasma was done as described above. For TMT, labeling samples were reconstituted in 100 mM TEAB for a final concentration of 1 μg/μl protein (53 μl for TMT six-plex, and 32 μl for TMT ten-plex). 21 μl and 12 μl of each of the TMT six-plex or TMT ten-plex reagent was added to the plasma aliquots, mixed and incubated at room temperature with shaking for 1 h. Three microliters of each sample was used to check label incorporation by LC-MS/MS prior to quenching the reactions. Reactions were quenched by adding 5% hydroxylamine at a 0.08 μl/μg concentration, dried down and desalted using Oasis HLB 1cc (30 mg) cartridges. Further processing of these samples was done as described below.

Fractionation of Peptides by Reversed Phase Chromatography at High pH (Basic pH RP)—Digested and iTRAQ labeled plasma sample for each patient was reconstituted in 540 μl of 20 mM ammonium formate/2% acetonitrile pH 10, loaded on a Zorbax 300 Extend 2.1 × 150 mm column (Agilent Technologies, Santa Clara, CA), and fractionated on an Agilent 1100 Series HPLC instrument by basic reversed-phase chromatography at a flow rate of 200 μl/min. Mobile phase consisted of 20 mM ammonium formate/2% acetonitrile pH 10 (buffer A) and 20 mM ammonium formate 90% acetonitrile pH 10 (buffer B). After loading 500 μl of sample (300 μg) onto the column, the peptides were separated using the following gradient: 5 min isocratic hold at 0% B, 0 to 15% solvent B in 8 min; 15 to 28.5% solvent B in 33 min; 28.5 to 34% solvent B in 5.5 min; 34 to 60% solvent B in 13 min, for a total gradient time of 64.5 min. Using 96 × 2 ml well plates, fractions were collected every 0.6 min for a total of 84 fractions through the main elution profile of the separation. In addition, the extreme early and late portions of the gradient were collected into two additional larger volume fractions. All fractions were acidified to a final concentration of 1% formic acid and the internal 84 fractions were then recombined by pooling early, mid and late fractions together resulting in a total of 28 fractions using concatenation strategy (3). These 28 fractions along with the additional 2 fractions representing early and late eluting peptides constructed a total of 30 fractions to be analyzed by LC-MS/MS. All fractions were dried to dryness by vacuum centrifugation and stored at −80 C until mass spectrometric analysis.

NanoLC-MS/MS analysis—For plasma samples from individual patients each of the 30 fractions was reconstituted in 16 μl of 5% formic acid/3% Acetonitrile and 2 μl were analyzed on Q Exactive mass spectrometer (Thermo Fisher Scientific) equipped with a nanoflow ionization source (James A. Hill Instrument Services, Arlington, MA) and coupled to an EASY-nLC 1000 UHPLC system (Thermo Fisher Scientific). Chromatography was performed on a 75 μm ID picofrit column (New Objective, Woburn, MA) packed in house with Reprosil-Pur C18 AQ 1.9 μm beads (Dr. Maisch, GmbH, Entringen, Germany) to a length of 20 cm. Columns were heated to 50°C using column heater sleeves (Phoenix-ST, Chester, PA) to prevent overpressuring of columns during UHPLC separation. The LC system, column, and platinum wire to deliver electrospray source voltage were connected via a stainless-steel cross (360 μm, IDEX Health & Science, UH-906x). Mobile phases consisted of 0.1% formic acid/3% acetonitrile as solvent A, and 0.1% formic acid/90% acetonitrile as solvent B. Peptides were eluted at 200 nL/min with a gradient of 6 to 35% B in 150 min, 35 to 60% B in 8 min, 60 to 90% B in 3 min, hold at 90% B for 10 min, 90% B to 50% B in 1 min, followed by isocratic conditions at 50% B for 10 min. A single Orbitrap MS scan from 300 to 1800 *m/z* at a resolution of 70,000 with AGC set at 3e6 was followed by up to 12 ms/ms scans at a resolution of 17,500 with AGC set at 5e4. MS/MS spectra were collected with normalized collision energy of 27 and isolation width of 2.5 amu. Dynamic exclusion was set to 20s, and peptide match was set to on.

For samples of plasma pooled from multiple patients and used in the iTRAQ/TMT comparison some of the above parameters were revised. Analyses were performed on a Q Exactive Plus mass spectrometer (Thermo Fisher Scientific) with an isolation width of 2.0 amu. For TMT labeled peptides the normalized collision energy was decreased to 26. For TMT-10 labeled peptides MS/MS spectra were collected at a resolution of 35,000.

Data Analysis—Data analysis was done using the Spectrum Mill MS Proteomics Workbench software package v 4.2 beta (Agilent Technologies). Similar MS/MS spectra acquired on the same precursor *m/z* within ± 60 s were merged. MS/MS spectra were excluded from searching if they failed the quality filter by not having a sequence tag length > 0 (*i.e.* minimum of two masses separated by the in-chain mass of an amino acid) or did not have a precursor MH+ in the range of 750–4000. All extracted spectra were searched against a UniProt database containing human reference proteome sequences (including isoforms and excluding fragments), 58,929 entries. The sequences were downloaded from the UniProt web site on October 17, 2014, redundant sequences removed, and a set of common labora-

tory contaminant proteins (150 sequences) appended. Search parameters included: ESI-QEXACTIVE-HCD-v2 scoring, parent and fragment mass tolerance of 20 ppm, 40% minimum matched peak intensity, trypsin allow P enzyme specificity with up to four missed cleavages, and calculate reversed database scores enabled. Fixed modifications were carbamidomethylation at cysteine. iTRAQ/TMT labeling was required at lysine, but peptide N termini were allowed to be either labeled or unlabeled. Allowed variable modifications were acetylation of protein N termini, oxidized methionine, deamidation of asparagine, pyro-glutamic acid at peptide N-terminal glutamine, and pyro-carbamidomethylation at peptide N-terminal cysteine with a precursor MH+ shift range of −18 to 70 Da. Database matches were autovalidated at the peptide and protein level in a two-step process with identification FDR estimated by target-decoy-based searches using reversed sequences. Peptide autovalidation was done first and separately for each patient directory of 30 LC-MS/MS files using an auto thresholds strategy with a minimum sequence length of six, automatic variable range precursor mass filtering, and score and delta Rank1 - Rank2 score thresholds optimized to yield a spectral level FDR estimate for precursor charges 2 thru 4 of <0.8% for each precursor charge state in each LC-MS/MS run. For precursor charge 5, thresholds were optimized to yield a spectral level FDR estimate of <0.4% across all runs per patient (instead of each run), to achieve reasonable statistics because many fewer spectra are generated for the higher charge state.

Protein polishing autovalidation, a feature of Spectrum Mill, was then applied using an auto thresholding strategy. Protein polishing determines the maximum protein level score of a protein group that consists entirely of distinct peptides estimated to be false-positive identifications (PSM's with negative delta forward-reverse scores). Then all PSM's contributing to protein groups with a score at or below this protein score threshold, or derived from only a single patient, are removed from the set of PSM's obtained in the initial peptide-level autovalidation step. This step further filters all the peptide-level validated spectra with the primary goal of eliminating peptides identified with low scoring peptide spectrum matches (PSM's) that represent proteins identified by a single peptide from a single patient, so-called one-hit wonders. Proteins were grouped together across the four patient directories with minimum number of directories set to 2; minimum protein score of 13 and maximum protein level FDR estimate of 0%. The protein polishing step filtered the results so that each identified protein is detected in more than one patient and is comprised of multiple peptides unless a single excellent scoring peptide was the sole match. As shown in Fig. 2, these settings yielded a spectrum level FDR estimate of <0.5% and a peptide level FDR estimate of <1.5% for each patient. In aggregate across all 4 patients the estimated FDR's are spectrum level: 0.45%, peptide level: 2.36%, and protein level: <0.02% (1/5304). Because the protein level FDR estimate neither explicitly requires a minimum number of distinct peptides per protein nor adjusts for the number of possible tryptic peptides per protein, it may underestimate false positive protein identifications for large proteins observed only on the basis of multiple low scoring PSM's.

In calculating scores at the protein level and reporting the identified proteins, redundancy is addressed in the following manner: the protein score is the sum of the scores of distinct peptides. A distinct peptide is the single highest scoring instance of a peptide detected through an MS/MS spectrum. MS/MS spectra for a particular peptide may have been recorded multiple times, (*i.e.* as different precursor charge states, in adjacent bRP fractions, or different modification states) but are still counted as a single distinct peptide. When a peptide sequence >8 residues long is contained in multiple protein entries in the sequence database, the proteins are grouped together and the highest scoring one and its accession number are reported. In some cases when the protein sequences are grouped in this manner there are distinct peptides which uniquely represent a lower scoring member of the group (isoforms, family members, or different species). Each of these instances spawns a subgroup and multiple subgroups are reported and counted toward the total number of proteins. Peptides shared between subgroups were counted toward each subgroup's count of distinct peptides and protein level iTRAQ/TMT quantitation. As listed in supplemental Table S2, assembly of confidently identified PSM's from all four patients into proteins yields 5340 total protein subgroups from 4591 protein groups. For further analyses in this study relying solely on identification the list was filtered to include only the 5304 protein subgroups identified by two or more peptides across all four patient samples. For quantitative analyses the list was filtered to include only the 4819 protein subgroups identified by two or more peptides in at least one patient sample.

Protein quantitation was done using iTRAQ/TMT ratios representing 10 min *versus* baseline, 1 h *versus* baseline, and 4 h *versus* baseline for each protein or different channels in iTRAQ/TMT comparison experiment. Spectrum Mill used the reporter ion intensities to calculate the iTRAQ/TMT ratios for each PSM. A protein level iTRAQ/TMT ratio was calculated as the median of all PSM level ratios contributing to the protein remaining after excluding those PSM's lacking an iTRAQ/TMT label, having a negative delta forward-reverse score (half of all false-positive identifications), or having a precursor ion purity <50% (MS/MS has significant precursor isolation contamination from co-eluting peptides).

Data Analysis of Spiked-in Peptides—After the first search and validation, unmatched spectra were searched against a Uniprot subset database containing only the proteins from which the unlabeled versions of the heavy labeled synthetic peptides would derive. Fixed modifications used for the search were iTRAQ, TMT6, or TMT10 labels at peptide N termini. Variable modifications were C13N15 Arginine, and iTRAQ, TMT6 or TMT10 labeled C13N15 Lysine at the C termini. iTRAQ and TMT ratios for the synthetic peptides were exported from Spectrum Mill and used for further analysis of iTRAQ, TMT6 and TMT10 spiked-in data.

Statistical Analysis—The moderated F-test was used to assess statistically significant changes over the time course in four PMI patient samples. The F-test was used to compare log2 transformed iTRAQ protein ratios from each of the three groups representing the 10 min *versus* baseline, 1 h *versus* baseline, and 4 h *versus* baseline comparisons to determine if any of the proteins in the groups have ratios statistically different from zero. Use of the F-test enables detection of arbitrary temporal patterns, and the moderated version of the test borrows information from all the observed proteins to assess variation of the ratios in a more robust manner. The moderated F-test is implemented in R (10) using the limma (11) library. Nominal *p* values determined by the test are corrected for multiple testing using the false discovery rate [FDR, (12)].

Scatter plots (Fig. 3) were generated to show iTRAQ ratios of each protein across pairs of patient samples, and time points. Statistically significant proteins (common across all scatter plots because they are determined using all patients and time points) are plotted in red.

The set of statistically significantly regulated proteins are grouped based on their temporal profile using fuzzy c-means clustering (Fig. 4) (13). The number of clusters is chosen based on visual inspection of cluster coherence and uniqueness of temporal profiles.

Sample Preparation for Verification Study Using ImmunoMRM (iMRM) Assay—

Plasma Digestion—Three out of the four PMI patients were included in the 23-plex immunoMRM assay. Thirty microliters plasma from baseline, 10, 60, and 240 min post-injury were digested in 3 process replicates on a Bravo Automated Liquid Handling Platform (Agilent Technologies). Briefly, plasma samples were added to a

96-well, 2 ml capacity plate and digested using the same protocol design as described earlier (14). To reduce evaporation, the plate was covered during the overnight period. The reactions were quenched by addition of formic acid to a final concentration of 1%. Prior to desalting, 100 fmol of isotopically labeled synthetic peptide standards were added to each well. Samples were then desalted using Oasis HLB 30 mg plate (Waters) on a Positive Pressure-96 Processor with the standard protocol as described previously. Samples were eluted in 80% acetonitrile/0.1% formic acid (3 × 500 μl) into a 2 ml capacity 96-well plate, frozen, vacuum centrifuged to dryness and stored at −80 °C.

Antibody Preparation—Anti-peptide antibodies were prepared as rabbit polyclonals by either Epitomics (Burlingame, CA) or New England Peptide (Gardner, MA) except for antibody against peptide TDPGVFIGVK (IL-33) which was prepared as a rabbit monoclonal. Antibodies incubated individually to 1 μm Dynabeads® Protein G (Life Technologies, Grand Island, NY) in batch mode mixing at 4 °C overnight. Beads were then transferred to wells in a KingFisher 96 Deepwell plate following protocol performed on the KingFisher 96 magnetic bead processor (Thermo Fisher Scientific Inc.): 30 min incubation with freshly made 20 mM dimethyl pimelimidate200 mM triethanolamine pH 8.5 followed by 30 min quenching step in 150 mM ethanolamine. Antibody Protein G conjugated beads were then washed twice for 5 min with 5% acetic acid/0.03% CHAPS followed by 5 min re-equilibration with 1X PBS/0.03% CHAPS. Antibody beads were finally resuspended in 1× PBS/0.03% CHAPS/0.1% NaN3 to 0.5 mg/ml and stored at 4 °C until use.

Peptide Immunoaffinity Enrichment—Each digested sample was resuspended in 210 μl of 1× PBS 0.01% CHAPS 100 mM Tris pH 8.0 and transferred to a 250 μl capacity 96-well plate. A mixture of 23 antipeptide antibodies cross-linked to beads was prepared and added to each well resulting in 1 μg of each conjugated antibody except for TPM.SID, FGL2.ELE and ITGB.GEV which were only 0.5 μg because of a limited supply. Samples were tumble-mixed overnight by tumble action at 4 °C. The next day, plates were transferred onto a KingFisher 96 magnetic particle processor and processed as described previously (15). Briefly, after mixing for 5 min on the KingFisher, the beads were washed twice with 1× PBS/0.0.3% CHAPS for 90 s followed by a third wash with 0.11× PBS/0.03% CHAPS for 90 s. Peptides were eluted from the antibody beads by mixing on KingFisher with 30 μl of 5% acetic acid/3% acetonitrile for 5 min. To eliminate possible bead transfer to the next phase of analysis (LC-MRM-MS), the elution plate (Bio-Rad Laboratories, Waltham, MA) was placed on a magnetic plate holder on wet ice and the contents of each well were transferred to a fresh plate, sealed with aluminum foil seal mat and stored at −80 °C until analysis.

LC-MRM-MS Analysis—Samples were reconstituted in 30 μl 0.1% formic acid/3% acetonitrile and 10 μl was analyzed on a 4000 Q Trap hybrid triple quadrupole, linear ion trap mass spectrometer equipped with Advanced Captive Spray MS source (Bruker, Auburn, CA) and coupled with an Eksigent Nano LC 2D Plus HPLC system (AB Sciex, Framingham, MA). Liquid chromatography conditions were described previously (15). Samples were analyzed on a 75 μm ID IntegraFrit column packed in-house to 10 cm with Reprosil-Pur C18 AQ 3 μm beads (Dr. Maisch, GmbH, Entringen, Germany) and connected to the spray tip of Captive Spray source. MS source parameters included source voltage of 1300, curtain and nebulizer gases of 0, interface heater temperature of 110 °C and collision gas set to medium. Three transitions per precursor were monitored with unit resolution for both Q1 and Q3. Declustering potential and collision energy were calculated for each precursor using the equations for 4000 Q Trap. Scheduled MRM method was used with 2 min retention time window and target cycle time of 0.9 s.

Data Analysis—Analysis of the data was done using Skyline open source software package (16). For each peptide light/heavy peak area ratio was used for further evaluation of results using QuaSAR (http://genepattern.broadinstitute.org/gp/pages/index.jsf?lsid = QuaSAR). Corresponding protein concentrations were calculated as described previously (15). Ten minutes *versus* baseline, 1 h *versus* baseline, and 4 h *versus* baseline protein concentration ratios were plotted to compare similar ratios calculated for iTRAQ reporter ions.

RESULTS

Improved Workflow Provides Faster, Deeper Discovery With More Precise Quantitation—To evaluate our plasma proteomic analysis workflow in the context of relevant biomarker discovery, four patients undergoing a therapeutic, PMI for hypertrophic cardiomyopathy were included in this study. Briefly, this planned injury model to ameliorate excess cardiac muscle in the interventricular septum recapitulates important features of spontaneous myocardial infarction, including the release of standard biomarkers (cardiac troponins) with the expected kinetics. The clinical characteristics of the patients are summarized in supplemental Table S1. Peripheral blood was collected from the patients at baseline (after catheter placement but before administration of alcohol into the coronary sinus) as well as at 10 min, 1 h, and 4 h after the induction of injury. The 16 total patient plasma samples were processed using the strategy shown in Fig. 1. The comprehensively revised workflow included numerous changes relative to our previous label-free approach (4), including changes to depletion, fractionation, on-line reversed phase chromatography, and MS instrumentation, in addition to the incorporation of iTRAQ labeling. In order to increase depth of detection in plasma, immunoaffinity depletion of abundant proteins is commonly employed (17–19). Here we used the IgY14/Supermix tandem depletion system (Sigma-Aldrich) prior to digestion and iTRAQ labeling of patient samples. The IgY14 antibody column removes the 14 most abundant plasma proteins including albumin, immunoglobulins G, A, and M, transferrin and others. The column flow-through is passed through the Supermix column, targeting 99% depletion of 50 moderate abundance proteins (though a larger number of proteins are captured at lower depletion efficiencies). Together these columns remove 96 to 99% of the total protein mass of plasma, promoting detection of low abundance proteins and allowing sampling of proteins present in plasma at low to sub-ng/ml levels (20, 21).

After abundant protein depletion and digestion, the samples were digested to peptides and labeled by iTRAQ fourplex reagent using a protocol optimized for plasma (see Methods). This chemical labeling strategy covalently modifies the primary amines of the N termini and Lysine side-chains of peptides (22). When iTRAQ-labeled peptides fragment in the mass spectrometer, distinct low *m/z* reporter ions are generated for each of the four different labels; relative quantification is based on ratios of these low *m/z* reporter ions. Incorporating iTRAQ labeling into the workflow allows mixing of four

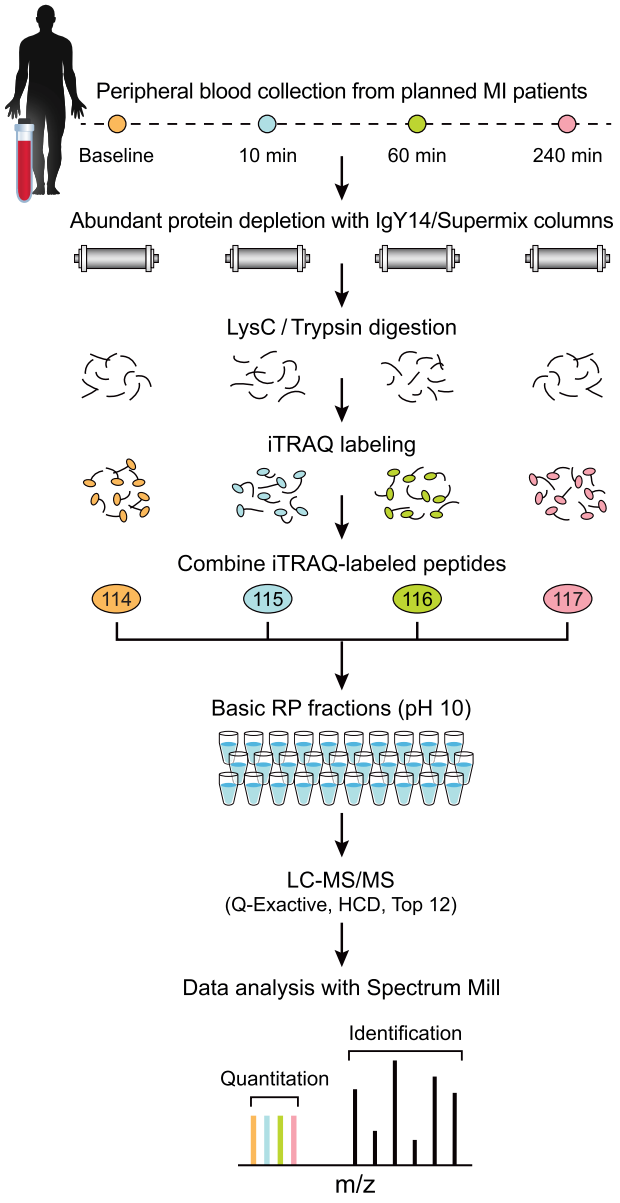

FIG. 1. **Diagram of improved workflow for discovery proteomics in plasma.** Samples from four different time points of planned MI (PMI) patients were depleted from abundant proteins, reduced, alkylated and digested by LysC/Trypsin. Following desalting, samples were labeled by four-plex iTRAQ reagent, and mixed after evaluating label incorporation. Sample was then fractionated using reversed phase chromatography at high pH into 30 pooled, concatenated fractions. Fractions were analyzed by data dependent analysis on a Q Exactive mass spectrometer using 75 μm picofrit columns packed in-house with 1.9 μm beads to 20 cm length. See Methods for details.

samples after the digestion step, reducing both pre-analytical and analytical variability and thereby providing more precise relative quantification of proteins compared with label-free methods (23, 24). iTRAQ-labeled peptides were fractionated offline using high pH reversed phase chromatography ("basic RP"). To improve orthogonality to the final on-line low pH RP separation, early, middle and late fractions were combined prior to LC-MS/MS analysis (2, 3). Basic reversed phase chromatography with concatenation of fractions has been shown to provide better resolution of iTRAQ-labeled peptides and phosphopeptides than SCX (25, 26). Thirty total fractions were analyzed by LC-MS/MS on 75 μm ID columns packed with sub-2 μm beads using a 150 min gradient (210 min inject-to-inject) and a latest generation Q Exactive mass spectrometer (Thermo Fisher Scientific). The combination of parallel time point analysis using iTRAQ and reduction of fraction number from 80 (SCX) to 30 (basic RP) more than offset the increase in effective gradient length (90 to 150 min), leading to more than a six-fold improvement in sample analysis speed and sample throughout compared with prior work (4).

Data were extracted and searched against the Uniprot Human database using Spectrum Mill software (Agilent). Up to 37,918 distinct peptides from an average of 4641 proteins (range 4280 - 4836) were identified in individual patient samples with a maximum peptide FDR estimate of $<$1.5% per patient (Fig. 2; see "Methods" for details). An aggregate total of 5,304 proteins were identified from at least two patients with at least two distinct peptides across the four patient samples with a protein FDR estimate of $<$0.02% (1/5304). An aggregate of 4819 proteins were further quantified by two or more peptides in at least one of the patient samples. supplemental Table S2 summarizes all proteins identified and quantified in the study. The list of identified peptides from all the proteins is presented in supplemental Table S3. Sixty four percent of the proteins (a total of 3390) were identified and quantified in all 16 samples from the four patients (Fig. 2). This represents nearly a five-fold increase in the depth of coverage of plasma proteome relative to our earlier label-free study (4), (supplemental Fig. S1). Importantly, the vast majority (ca. 85%) of proteins detected in our previous study were rediscovered in the present study.

To assess the improvement in depth of coverage that was specifically attributable to the additional depletion of moderately abundant plasma proteins by Supermix, we compared IgY14 depletion to IgY14/Supermix tandem depletion for a subset of 12 samples from three patients. Approximately 2800 total proteins were identified and quantified (with two or more distinct peptides/protein) in aggregate across the twelve samples using IgY14 depletion alone. In contrast, nearly 5100 proteins were detected and quantified in the same twelve samples using IgY14/Supermix depletion (supplemental Table S4, supplemental Fig. S1*B*). Therefore, the additional depletion of moderately abundant plasma proteins alone increases global proteome coverage by 82%. Further depletion does not however create a strict superset: 402 proteins most of which were identified and quantified by two–eight distinct peptides in at least one patient sample after IgY14 depletion alone were not detected after tandem IgY14/Supermix depletion (supplemental Table S5). Forty-six out of the 402 proteins

	Total Spectra	FDR Spectra (%)	Distinct Peptides	FDR Distinct Peptide (%)	Protein Subgroups Identified[a]	Protein Subgroups Quantified[b]
Patient 1	169295	0.43	37918	1.29	4836	4464
Patient 2	173378	0.47	36186	1.49	4780	4425
Patient 3	165812	0.45	35981	1.42	4670	4335
Patient 4	126050	0.45	28843	1.26	4280	4002
Overall	634535	0.45	54742	2.36	5304 (4555[c])	4819 (4105[c])

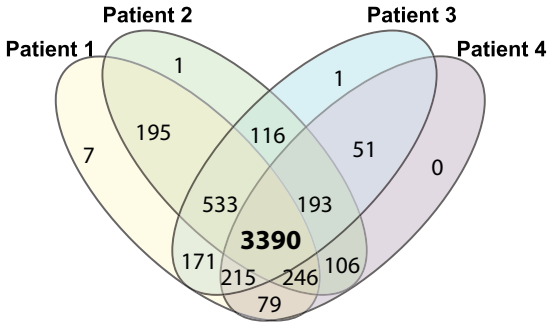

FIG. 2. **Identification summary statistics in the four PMI patient samples.** Table enumerates the number of spectra collected, distinct peptides and proteins identified along with the FDR values achieved in four PMI patient samples as reported by Spectrum Mill (see "Methods" for details). Venn diagram shows the overlap of proteins quantified in four PMI patient samples. [a]Proteins identified in at least two patients with two or more peptides. [b]Subset of identified proteins with two or more distinct peptides observed in at least one patient. [c]Protein subgroups (groups); that is, 5304 distinct protein subgroups were identified within 4555 protein groups. Proteins that share a detected distinct peptide (length >8) are combined into a group. A protein group is parsimoniously expanded to one or more subgroups to distinguish proteins that also have one or more distinct peptides that are not shared with the rest of the group, typically isoforms and family members.

were detected in the Supermix bound fraction of the same three patient samples.

The normalized mean intensities of proteins observed and quantified across the 16 plasma samples after IgY14/Supermix depletion span nine orders of magnitude (supplemental Figs. S2 and S3 and supplemental Table S6). It is noteworthy that cardiac troponins I and T, which are known to be at low abundance in plasma at early time points after myocardial injury (typically picogram/mL), are robustly detected and quantified in all patient samples with up to 6–8 peptides observed for each troponin (supplemental Table S7). In contrast, cardiac Troponin T was observed only sporadically and with only a single peptide in our prior label-free study (4), whereas Troponin I was not observed at all. Of note, no peptides from cardiac troponins were detected by the current workflow in samples depleted with IgY14 alone (data not shown).

iTRAQ Detects Novel Candidate Biomarkers of MI—In our experimental design, patients served as their own controls, with data reported as iTRAQ ratios between the 10 min, 1 h and 4 h post-injury timepoints *versus* the pre-injury baseline. Quantification was based on the median ratio of all peptides quantified for each protein, as reported by Spectrum Mill (see "Methods"). To facilitate comparison, data for each iTRAQ channel (representing a specific patient and time point) were median centered, that is, ratios for all proteins were normalized to the median ratio for that channel. A moderated F-test was used to assess statistically significant changes in abundance of the 4819 proteins detected and quantified with two or more peptides in at least one of the patient samples (see Methods). Selected examples of the resulting scatter plots are shown in Fig. 3. A total of 333 proteins were significantly regulated over the time course (meaning relative protein abundance differed significantly from baseline at least in one post-injury time point) with a Benjamini-Hochberg corrected p value of less than 0.05 (Table I). The number of confidently regulated proteins is six times larger than in our previous study (4). Levels for 90% of the 333 regulated proteins increased as a result of cardiac injury, whereas the levels for only 38 proteins decreased following the injury. Established markers of myocardial injury including myoglobin (MB), creatine kinase B (CKB), creatine kinase M (CKM), fatty acid binding protein (FABP) and all Troponins (TNNT2, TNNI3, TNNC1, and TNNC2) were in the up-regulated list and showed consistent behavior across the different patients (27).

Fuzzy c-means clustering of the 333 regulated proteins revealed five distinct clusters comprised of 323 of the proteins (Fig. 4, Table I). Cluster 1 represents those proteins that peak at 10 min post-injury. Cluster 2 consists of proteins that continue to increase from 10 min to 1 h and then plateau, whereas cluster 3 consists of those proteins that begin to decline after 1 h. Proteins that rise continuously throughout the time course comprise cluster 4, and those proteins that decline after injury are represented by cluster 5. Clustering in the present study recapitulates the temporal behavior of reg-

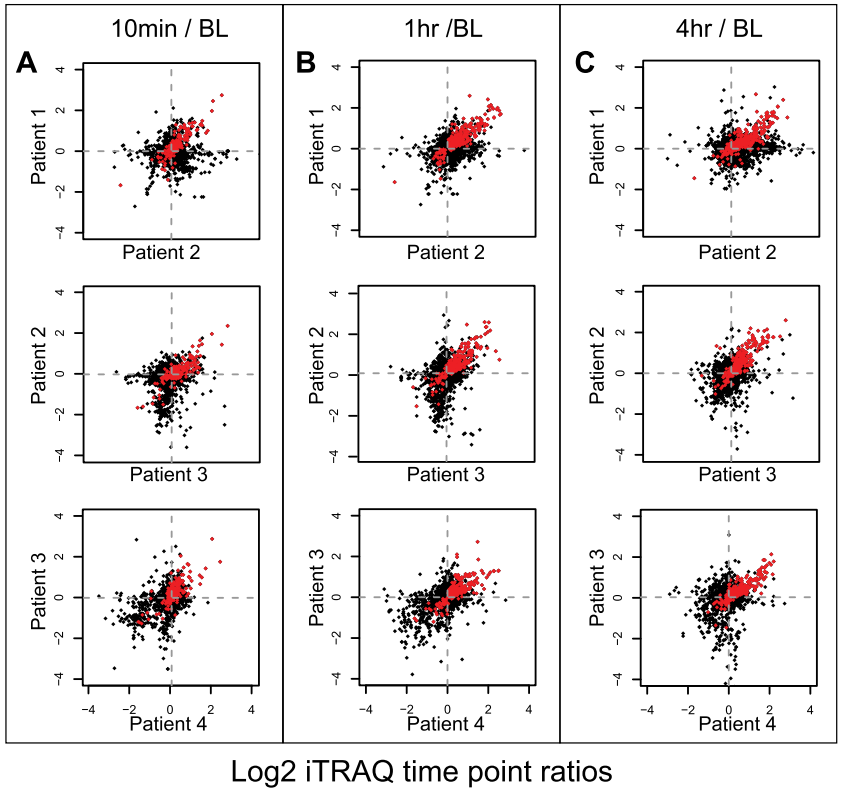

FIG. 3. **Scatter plots of protein iTRAQ ratios.** Protein iTRAQ ratios are plotted for a representative set of two patients for 10 min *versus* baseline (*A*), 1 h *versus* baseline (*B*), and 4 h *versus* baseline (*C*). Red dots indicate statistically significant proteins using moderated F-test with Benjamini-Hochberg corrected p value < 0.05 and these proteins are common across all scatter plots because they are determined using all patients and time points.

ulated proteins observed in our previous study (4), such as ACLP1 and PF4V1 peaking at 10 min (cluster 1), and FHL1 and MYL3 rising more slowly (clusters 2 and 3). Troponins showed the expected temporal profiles, with TNNT2, TNNI3, and TNNC1 belonging to cluster 4 and showing continuously increasing levels up to the 4 h time point. The vast majority of differential regulated proteins identified are candidate markers for early myocardial injury, showing elevation at 10 min that persists until at least 60 min after injury. Using the list of regulated proteins sorted by the cluster number we generated a heat map to investigate protein changes at individual patient level (supplemental Fig. S4). Importantly, consistent changes are observed for most of the proteins across the different time points and patients, suggesting (despite small sample numbers) that candidate markers may be uniform across the population.

iTRAQ Can Provide Highly Reproducible Quantification in Plasma Despite Ratio Compression—To assess the reproducibility of iTRAQ quantification as well as the extent of ratio compression we spiked heavy-labeled synthetic peptides at different concentrations into 4 iTRAQ channels corresponding to the four time point samples of PMI patients prior to iTRAQ labeling. An amount predicted to be at the detection threshold was spiked into the first channel, with the remaining channels were spiked with relative ratios of 2:1, 5:1, and 10:1. Results from 97 synthetic peptides are summarized in supplemental Fig. S5. Median iTRAQ ratios were compressed up to 50% in depleted plasma *versus* theoretical values, with compression being nonlinear; there was increased relative compression at higher relative ratios, consistent with prior studies in cell lysates (28, 29). We also assessed the reproducibility of quantification incorporating iTRAQ labeling using the data from 97 peptides. This was accomplished by performing the 4-channel spike-in experiment (described above) in replicate using the four different time point samples from each of 3 different patients. The median CVs ranged from 16 to 24% for the 3 different peptide spike level ratios tested.

Further Increases in Multiplexing of Plasma Analysis can be Successfully Achieved Using TMT-Labeling—Next, we tested whether TMT isobaric labeling reagents could further enhance throughput for discovery proteomics in plasma. Pooled normal plasma from a commercial source (BioreclamationIVT, Baltimore, MD) was depleted and digested as described. The total amount of digested plasma protein used in each labeling plex was kept constant at 360 μg; that amount was divided by 4, 6, or 10 (*i.e.* 80 μg, 53.3 μg, and 32 μg) for each labeling channel of iTRAQ four-plex, TMT six-plex and TMT ten-plex, respectively. All reporter ion channels contained equal amounts of the same plasma sample within an experiment to allow an unbiased assessment of total protein and peptide level coverage. The number of distinct peptides decreased by ~17% in both TMT six-plex and ten-plex experiments relative to the iTRAQ four-plex experiment (supplemental Fig. S6). Only 9% fewer proteins were detected in the TMT six-plex study and 17% fewer were detected in theTMT ten-plex experiment as compared with the iTRAQ four-plex experiment. These results

TABLE I
List of 333 regulated proteins in 4 PMI patient samples using iTRAQ workflow

Uniprot accession number	Gene symbol	Protein name	Log2 iTRAQ ratio (average of 4 PMI patients)			Moderated F-test *p* value[a]	Cluster[b]
			10min vs. BL	1hr vs. BL	4hr vs. BL		
Q9UPZ6	THSD7A	Thrombospondin type-1 domain-containing protein 7A	0.907	0.755	0.022	2.06E-05	1
Q9C0I4	THSD7B	Thrombospondin type-1 domain-containing protein 7B	0.669	0.574	0.040	8.12E-03	1
Q8IUX7	AEBP1	Adipocyte enhancer-binding protein 1	1.215	0.868	−0.082	1.17E-03	1
Q8N436	CPXM2	Inactive carboxypeptidase-like protein X2	1.986	1.447	−0.234	2.28E-02	1
Q02818	NUCB1	Nucleobindin-1	0.713	0.571	−0.050	1.09E-02	1
P05164–3	MPO	Isoform H7 of Myeloperoxidase	0.924	0.760	0.116	1.21E-04	1
P19801–2	AOC1	Isoform 2 of Amiloride-sensitive amine oxidase [copper-containing]	1.383	1.298	0.155	2.06E-05	1
P02549	SPTA1	Spectrin alpha chain, erythrocytic 1	0.408	0.405	0.209	6.68E-03	1
Q12906–7	ILF3	Isoform 7 of Interleukin enhancer-binding factor 3	0.180	0.169	0.054	4.45E-02	1
P11150	LIPC	Hepatic triacylglycerol lipase	1.186	1.347	0.150	5.93E-05	1
P19883	FST	Follistatin	1.187	0.944	0.019	3.59E-05	1
P08294	SOD3	Extracellular superoxide dismutase [Cu-Zn]	0.702	0.579	0.011	5.07E-03	1
Q8N474	SFRP1	Secreted frizzled-related protein 1	1.372	0.901	0.081	8.71E-05	1
P80303–2	NUCB2	Isoform 2 of Nucleobindin-2	0.518	0.448	0.133	1.02E-02	1
P21741	MDK	Midkine	2.341	1.655	0.208	1.21E-04	1
P10646	TFPI	Tissue factor pathway inhibitor	0.474	0.523	−0.025	4.28E-02	1
O95631	NTN1	Netrin-1	0.799	0.641	0.121	8.03E-04	1
P25940	COL5A3	Collagen alpha-3(V) chain	0.547	0.365	0.019	3.96E-02	1
P21246	PTN	Pleiotrophin	2.209	1.906	0.338	1.11E-04	1
P02776	PF4	Platelet factor 4	1.308	1.251	0.413	2.81E-02	1
P10720	PF4V1	Platelet factor 4 variant	1.261	1.149	0.415	2.09E-02	1
P20827	EFNA1	Ephrin-A1	0.360	0.355	0.045	1.83E-02	1
Q9BY76	ANGPTL4	Angiopoietin-related protein 4	0.609	0.397	0.229	2.50E-02	1
Q15109–3	AGER	Isoform 3 of Advanced glycosylation end product-specific receptor	0.553	0.366	−0.040	2.97E-02	1
O43508	TNFSF12	Tumor necrosis factor ligand superfamily member 12	0.714	0.467	−0.064	4.95E-02	1
P02788	LTF	Lactotransferrin	0.329	0.210	0.140	2.09E-02	1
Q99584	S100A13	Protein S100-A13	1.131	1.003	0.126	9.07E-03	1
P18827	SDC1	Syndecan-1	0.312	0.297	0.175	5.58E-03	1
O95969	SCGB1D2	Secretoglobin family 1D member 2	1.302	0.359	0.369	3.40E-02	1
E7EN11	CACNB4	Voltage-dependent L-type calcium channel subunit beta-4	0.497	0.377	0.333	2.65E-02	1
P04040	CAT	Catalase	0.090	0.312	0.360	3.96E-02	2
Q13228–4	SELENBP1	Isoform 4 of Selenium-binding protein 1	0.050	0.246	0.294	4.76E-02	2
P00558	PGK1	Phosphoglycerate kinase 1	0.172	0.643	0.709	4.54E-04	2
P48147	PREP	Prolyl endopeptidase	0.113	0.394	0.408	2.75E-03	2
P07951–2	TPM2	Isoform 2 of Tropomyosin beta chain	0.338	0.549	0.517	6.83E-03	2
P07951	TPM2	Tropomyosin beta chain	0.316	0.510	0.462	2.70E-02	2
P06733	ENO1	Alpha-enolase	0.112	0.262	0.340	1.81E-02	2
P02144	MB	Myoglobin	0.790	1.939	1.506	2.03E-04	2
P68082	MB	Myoglobin	0.710	1.970	1.533	5.12E-04	2
P04406	GAPDH	Glyceraldehyde-3-phosphate dehydrogenase	0.141	0.729	0.729	2.22E-02	2
P60174	TPI1	Triosephosphate isomerase	0.345	1.067	0.893	8.03E-04	2
P60174–4	TPI1	Isoform 4 of Triosephosphate isomerase	0.327	1.110	0.923	1.17E-03	2
P63104	YWHAZ	14–3-3 protein zeta/delta	0.241	0.433	0.458	8.41E-03	2
P31946–2	YWHAB	Isoform Short of 14–3-3 protein beta/alpha	0.157	0.388	0.313	3.94E-03	2
Q04917	YWHAH	14–3-3 protein eta	0.195	0.422	0.483	1.52E-03	2
P27348	YWHAQ	14–3-3 protein theta	0.156	0.368	0.394	9.83E-04	2
P31947	SFN	14–3-3 protein sigma	0.191	0.427	0.542	3.55E-04	2
P28838	LAP3	Cytosol aminopeptidase	0.166	0.562	0.633	2.12E-02	2
E7EQ12	CAST	Calpastatin	0.153	0.434	0.554	2.26E-03	2
P15259	PGAM2	Phosphoglycerate mutase 2	0.294	1.157	1.388	2.08E-04	2
P61158	ACTR3	Actin-related protein 3	0.154	0.248	0.255	1.66E-02	2
P05413	FABP3	Fatty acid-binding protein, heart	0.615	1.831	1.851	1.13E-04	2
P40926	MDH2	Malate dehydrogenase, mitochondrial	0.747	1.976	1.374	1.21E-04	2
Q5JRA6	MIA3	Melanoma inhibitory activity protein 3	0.308	0.506	0.443	6.73E-04	2
P23526	AHCY	Adenosylhomocysteinase	0.182	0.477	0.435	1.93E-03	2
P15121	AKR1B1	Aldose reductase	0.276	1.009	0.778	8.03E-04	2
P35237	SERPINB6	Serpin B6	0.050	0.225	0.204	1.08E-02	2
Q5T4U5	ACADM	Acyl-Coenzyme A dehydrogenase, C-4 to C-12 straight chain, isoform CRA_a	0.452	1.138	1.259	1.17E-03	2
O15143	ARPC1B	Actin-related protein 2/3 complex subunit 1B	0.145	0.291	0.262	3.00E-02	2
P07738	BPGM	Bisphosphoglycerate mutase	0.136	0.337	0.327	2.26E-02	2
Q9HC38–2	GLOD4	Isoform 2 of Glyoxalase domain-containing protein 4	0.059	0.323	0.342	2.86E-02	2
Q9HC38	GLOD4	Glyoxalase domain-containing protein 4	0.059	0.337	0.342	3.19E-02	2
B7Z403	GLOD4	Glyoxalase domain-containing protein 4	0.066	0.324	0.329	3.00E-02	2
P61160	ACTR2	Actin-related protein 2	0.149	0.248	0.276	2.15E-02	2

TABLE I—*continued*

Uniprot accession number	Gene symbol	Protein name	Log2 iTRAQ ratio (average of 4 PMI patients)			Moderated F-test *p* value[a]	Cluster[b]
			10min vs. BL	1hr vs. BL	4hr vs. BL		
P10768	ESD	S-formylglutathione hydrolase	0.141	0.550	0.610	1.23E-03	2
Q8N142	ADSSL1	Adenylosuccinate synthetase isozyme 1	0.125	1.054	1.038	1.72E-02	2
Q9UJ70	NAGK	N-acetyl-D-glucosamine kinase	0.048	0.261	0.202	2.65E-02	2
P54727	RAD23B	UV excision repair protein RAD23 homolog B	0.102	0.299	0.389	2.26E-03	2
P30086	PEBP1	Phosphatidylethanolamine-binding protein 1	0.256	0.877	0.553	5.07E-03	2
Q99497	PARK7	Protein DJ-1	0.059	0.439	0.511	4.01E-03	2
Q13011	ECH1	Delta(3,5)-Delta(2,4)-dienoyl-CoA isomerase, mitochondrial	0.300	1.433	1.186	1.99E-03	2
P00492	HPRT1	Hypoxanthine-guanine phosphoribosyltransferase	0.123	0.355	0.365	1.06E-03	2
Q32Q12	NME1-NME2	Nucleoside diphosphate kinase	0.112	0.447	0.305	2.81E-03	2
P15531–2	NME1	Isoform 2 of Nucleoside diphosphate kinase A	0.114	0.430	0.359	2.75E-03	2
F6XY72	NME1-NME2	Protein NME1-NME2	0.078	0.456	0.269	1.53E-03	2
Q9UL46	PSME2	Proteasome activator complex subunit 2	0.106	0.316	0.342	4.57E-02	2
Q16836–2	HADH	Isoform 2 of Hydroxyacyl-coenzyme A dehydrogenase, mitochondrial	0.542	1.898	1.485	2.03E-04	2
Q13642–4	FHL1	Isoform 4 of Four and a half LIM domains protein 1	0.235	0.841	0.642	1.98E-04	2
P62805	HIST1H4A	Histone H4	0.631	1.166	1.441	7.14E-05	2
Q8TDQ7	GNPDA2	Glucosamine-6-phosphate isomerase 2	0.097	0.234	0.291	1.57E-02	2
P46926	GNPDA1	Glucosamine-6-phosphate isomerase 1	0.154	0.417	0.445	4.17E-03	2
Q96DG6	CMBL	Carboxymethylenebutenolidase homolog	0.160	0.833	0.749	2.21E-02	2
P59998	ARPC4	Actin-related protein 2/3 complex subunit 4	0.175	0.415	0.350	2.12E-02	2
P00441	SOD1	Superoxide dismutase [Cu-Zn]	0.168	0.629	0.448	2.12E-02	2
P49247	RPIA	Ribose-5-phosphate isomerase	0.071	0.215	0.200	2.04E-02	2
P02689	PMP2	Myelin P2 protein	0.296	0.822	0.824	1.98E-02	2
Q96C23	GALM	Aldose 1-epimerase	0.047	0.381	0.472	4.08E-02	2
P29218	IMPA1	Inositol monophosphatase 1	0.174	0.679	0.874	8.74E-04	2
P30042	C21orf33	ES1 protein homolog, mitochondrial	0.409	1.330	1.248	1.11E-03	2
Q15631	TSN	Translin	0.164	0.334	0.367	5.07E-03	2
O00764	PDXK	Pyridoxal kinase	0.113	0.800	0.780	2.49E-02	2
P63208	SKP1	S-phase kinase-associated protein 1	0.095	0.434	0.352	2.38E-02	2
O15145	ARPC3	Actin-related protein 2/3 complex subunit 3	0.160	0.350	0.326	2.36E-02	2
Q04760	GLO1	Lactoylglutathione lyase	0.287	0.742	0.523	2.29E-03	2
P06734	FCER2	Low affinity immunoglobulin epsilon Fc receptor	0.130	0.184	0.188	4.45E-02	2
P07108	DBI	Acyl-CoA-binding protein	0.221	0.688	0.523	1.18E-02	2
P50461	CSRP3	Cysteine and glycine-rich protein 3	0.359	1.504	1.617	5.93E-05	2
U3KQK0	HIST1H2BN	Histone H2B	0.522	1.251	1.556	2.06E-05	2
P33778	HIST1H2BB	Histone H2B type 1-B	0.582	1.259	1.606	4.41E-05	2
Q99880	HIST1H2BL	Histone H2B type 1-L	0.536	1.269	1.573	2.06E-05	2
P30048	PRDX3	Thioredoxin-dependent peroxide reductase, mitochondrial	0.085	0.882	1.013	7.43E-03	2
O95861–2	BPNT1	Isoform 2 of 3′(2′),5′-bisphosphate nucleotidase 1	0.092	0.478	0.458	1.41E-03	2
O75347	TBCA	Tubulin-specific chaperone A	0.020	0.296	0.261	4.86E-02	2
P84243	H3F3A	Histone H3.3	0.584	1.241	1.502	2.03E-04	2
P68431	HIST1H3A	Histone H3.1	0.570	1.181	1.411	5.93E-05	2
Q71DI3	HIST2H3A	Histone H3.2	0.648	1.256	1.506	2.08E-04	2
Q5TEC6	HIST2H3PS2	Histone H3	0.467	1.084	1.322	7.20E-04	2
P10644	PRKAR1A	cAMP-dependent protein kinase type I-alpha regulatory subunit	0.105	0.311	0.321	2.12E-02	2
Q9NR45	NANS	Sialic acid synthase	0.106	0.312	0.388	1.61E-02	2
Q9H0R4	HDHD2	Haloacid dehalogenase-like hydrolase domain-containing protein 2	0.179	0.619	0.773	5.11E-03	2
P61970	NUTF2	Nuclear transport factor 2	0.044	0.343	0.218	3.53E-02	2
Q9NVS9	PNPO	Pyridoxine-5′-phosphate oxidase	0.182	0.407	0.419	3.45E-02	2
Q12765–2	SCRN1	Isoform 2 of Secernin-1	0.092	0.234	0.282	2.63E-02	2
Q6FI13	HIST2H2AA3	Histone H2A type 2-A	0.665	1.483	1.843	3.17E-04	2
Q7L7L0	HIST3H2A	Histone H2A type 3	0.667	1.497	1.843	2.99E-04	2
P0C0S5	H2AFZ	Histone H2A.Z	0.799	1.522	1.934	2.79E-03	2
P23297	S100A1	Protein S100-A1	0.977	1.678	1.967	6.15E-04	2
O15511	ARPC5	Actin-related protein 2/3 complex subunit 5	0.209	0.283	0.324	2.76E-02	2
P35754	GLRX	Glutaredoxin-1	0.040	0.316	0.279	2.24E-03	2
Q9NRX4	PHPT1	14 kDa phosphohistidine phosphatase	0.144	0.450	0.296	1.66E-02	2
Q99729	HNRNPAB	Heterogeneous nuclear ribonucleoprotein A/B	0.117	0.240	0.264	3.18E-02	2
Q14061	COX17	Cytochrome c oxidase copper chaperone	0.858	1.712	1.342	2.08E-04	2
Q7Z4H3	HDDC2	HD domain-containing protein 2	0.089	0.569	0.518	2.51E-03	2
Q99471	PFDN5	Prefoldin subunit 5	0.265	0.605	0.500	4.92E-03	2
P14621	ACYP2	Acylphosphatase-2	0.198	0.696	0.607	8.97E-03	2
U3KQL2	ACYP2	Acylphosphatase-2	0.212	0.570	0.520	7.64E-03	2
Q07507	DPT	Dermatopontin	0.454	0.749	0.654	2.27E-02	2

TABLE I—*continued*

Uniprot accession number	Gene symbol	Protein name	Log2 iTRAQ ratio (average of 4 PMI patients)			Moderated F-test *p* value[a]	Cluster[b]
			10min vs. BL	1hr vs. BL	4hr vs. BL		
B7Z4W5	CCBL1	Cysteine conjugate-beta lyase cytoplasmic (Glutamine transaminase K, kyneurenine aminotransferase), isoform CRA_b	−0.037	0.687	0.810	3.24E-02	2
Q9UHP9	SMPX	Small muscular protein	0.464	0.643	0.659	9.28E-03	2
P07919	UQCRH	Cytochrome b-c1 complex subunit 6, mitochondrial	0.674	1.897	1.652	9.22E-03	2
P49789	FHIT	Bis(5′-adenosyl)-triphosphatase	0.050	1.026	0.608	2.49E-02	2
Q0VDG4	SCRN3	Secernin-3	0.246	0.433	0.566	2.79E-03	2
Q86YS3	RAB11FIP4	Rab11 family-interacting protein 4	0.208	0.811	0.652	9.67E-03	2
Q9ULP9	TBC1D24	TBC1 domain family member 24	0.060	0.602	0.722	5.95E-03	2
Q9BPX5	ARPC5L	Actin-related protein 2/3 complex subunit 5-like protein	0.185	0.559	0.555	2.22E-02	2
O14561	NDUFAB1	Acyl carrier protein, mitochondrial	0.298	1.098	1.348	3.93E-03	2
O75369–8	FLNB	Isoform 8 of Filamin-B	0.227	0.328	0.285	1.01E-03	3
Q00610	CLTC	Clathrin heavy chain 1	0.308	0.441	0.228	4.08E-02	3
J3KN67	TPM3	Tropomyosin alpha-3 chain	0.457	0.520	0.322	4.52E-02	3
P06753–6	TPM3	Isoform 6 of Tropomyosin alpha-3 chain	0.469	0.524	0.313	3.96E-02	3
P06753–5	TPM3	Isoform 5 of Tropomyosin alpha-3 chain	0.472	0.526	0.306	4.24E-02	3
P48735	IDH2	Isocitrate dehydrogenase [NADP], mitochondrial	0.874	2.055	0.978	2.16E-04	3
P08670	VIM	Vimentin	0.261	0.356	0.236	4.92E-03	3
P07196	NEFL	Neurofilament light polypeptide	0.203	0.324	0.246	2.50E-02	3
Q96G03	PGM2	Phosphoglucomutase-2	0.121	0.358	0.078	3.00E-02	3
Q06830	PRDX1	Peroxiredoxin-1	0.145	0.420	0.258	4.56E-02	3
B1AVU8	PSAP	Saposin-D	0.162	0.191	0.094	5.99E-03	3
P07602–3	PSAP	Isoform Sap-mu-9 of Prosaposin	0.164	0.212	0.095	5.11E-03	3
P21709	EPHA1	Ephrin type-A receptor 1	0.182	0.277	0.121	4.30E-02	3
Q16555	DPYSL2	Dihydropyrimidinase-related protein 2	0.104	0.181	0.075	4.27E-02	3
Q14194–2	CRMP1	Isoform LCRMP-1 of Dihydropyrimidinase-related protein 1	0.151	0.277	0.125	3.45E-02	3
P23284	PPIB	Peptidyl-prolyl cis-trans isomerase B	0.165	0.270	0.147	3.14E-02	3
P08590	MYL3	Myosin light chain 3	1.198	1.510	0.843	1.81E-04	3
P12829	MYL4	Myosin light chain 4	1.062	1.285	0.533	7.30E-03	3
P07585	DCN	Decorin	0.556	0.760	0.456	2.03E-04	3
P62937	PPIA	Peptidyl-prolyl cis-trans isomerase A	0.103	0.361	0.167	3.55E-03	3
P62937–2	PPIA	Isoform 2 of Peptidyl-prolyl cis-trans isomerase A	0.089	0.344	0.145	7.81E-03	3
Q9Y625	GPC6	Glypican-6	0.217	0.365	0.210	7.29E-03	3
P21810	BGN	Biglycan	0.715	0.887	0.458	2.16E-04	3
P62158	CALM1	Calmodulin	0.231	0.435	0.161	7.64E-03	3
P09211	GSTP1	Glutathione S-transferase P	0.089	0.363	0.169	1.58E-02	3
P19338	NCL	Nucleolin	0.281	0.481	0.380	2.21E-02	3
Q9BRF8	CPPED1	Serine/threonine-protein phosphatase CPPED1	0.215	0.518	0.305	7.44E-03	3
P03950	ANG	Angiogenin	0.166	0.318	0.166	3.53E-02	3
Q9UBQ0	VPS29	Vacuolar protein sorting-associated protein 29	0.203	0.503	0.243	2.67E-02	3
P12104	FABP2	Fatty acid-binding protein, intestinal	0.265	0.438	0.092	9.69E-03	3
Q9NQ30	ESM1	Endothelial cell-specific molecule 1	0.705	0.956	0.747	2.08E-04	3
P50897	PPT1	Palmitoyl-protein thioesterase 1	0.153	0.373	0.088	4.45E-03	3
P36543	ATP6V1E1	V-type proton ATPase subunit E 1	0.224	0.269	0.245	2.71E-02	3
P30405	PPIF	Peptidyl-prolyl cis-trans isomerase F, mitochondrial	0.644	1.610	0.612	4.01E-03	3
P20674	COX5A	Cytochrome c oxidase subunit 5A, mitochondrial	1.036	1.534	0.594	1.11E-02	3
Q09028	RBBP4	Histone-binding protein RBBP4	0.317	0.671	0.315	4.27E-02	3
P02585	TNNC2	Troponin C, skeletal muscle	0.519	0.607	0.274	2.12E-02	3
O43447	PPIH	Peptidyl-prolyl cis-trans isomerase H	0.125	0.359	0.195	2.12E-02	3
Q96G01	BICD1	Protein bicaudal D homolog 1	0.332	0.427	0.331	2.65E-02	3
O75380	NDUFS6	NADH dehydrogenase [ubiquinone] iron-sulfur protein 6, mitochondrial	0.377	1.066	0.656	2.12E-02	3
P18206	VCL	Vinculin	0.102	0.211	0.438	1.88E-03	4
P26038	MSN	Moesin	0.065	0.168	0.264	1.26E-02	4
P15311	EZR	Ezrin	0.026	0.203	0.443	1.11E-02	4
P35241–5	RDX	Isoform 5 of Radixin	0.070	0.253	0.419	7.64E-03	4
P11216	PYGB	Glycogen phosphorylase, brain form	0.133	0.469	0.791	4.01E-03	4
P34932	HSPA4	Heat shock 70 kDa protein 4	0.039	0.126	0.297	1.02E-02	4
P11142	HSPA8	Heat shock cognate 71 kDa protein	0.111	0.419	0.729	2.58E-04	4
P08107	HSPA1A	Heat shock 70 kDa protein 1A/1B	0.095	0.444	0.760	6.71E-04	4
P17066	HSPA6	Heat shock 70 kDa protein 6	0.138	0.559	0.885	2.45E-04	4
P14618–2	PKM	Isoform M1 of Pyruvate kinase PKM	0.075	0.401	0.910	2.03E-04	4
P14618	PKM	Pyruvate kinase PKM	0.077	0.381	0.880	2.32E-04	4
P06732	CKM	Creatine kinase M-type	0.260	1.108	1.827	5.93E-05	4
P12277	CKB	Creatine kinase B-type	0.273	1.113	1.760	5.93E-05	4
P31150	GDI1	Rab GDP dissociation inhibitor alpha	0.065	0.159	0.257	7.26E-03	4
P04075–2	ALDOA	Isoform 2 of Fructose-bisphosphate aldolase A	−0.015	0.204	0.547	4.89E-04	4

TABLE I—*continued*

Uniprot accession number	Gene symbol	Protein name	Log2 iTRAQ ratio (average of 4 PMI patients)			Moderated F-test *p* value[a]	Cluster[b]
			10min vs. BL	1hr vs. BL	4hr vs. BL		
P09972	ALDOC	Fructose-bisphosphate aldolase C	−0.019	0.128	0.527	5.42E-03	4
P36871	PGM1	Phosphoglucomutase-1	0.086	0.581	1.139	8.28E-04	4
P06744	GPI	Glucose-6-phosphate isomerase	0.221	0.859	1.331	4.88E-04	4
P00338	LDHA	L-lactate dehydrogenase A chain	0.075	0.192	0.383	2.21E-02	4
P07195	LDHB	L-lactate dehydrogenase B chain	0.051	0.243	0.694	7.48E-04	4
P07864	LDHC	L-lactate dehydrogenase C chain	0.087	0.299	0.639	1.60E-03	4
P52209	PGD	6-phosphogluconate dehydrogenase, decarboxylating	0.083	0.269	0.385	1.78E-02	4
Q6ZN40	TPM1	Tropomyosin 1 (Alpha), isoform CRA_f	0.321	0.642	0.940	2.57E-04	4
H0YK48	TPM1	Tropomyosin alpha-1 chain	0.325	0.614	0.892	1.93E-03	4
P09493–4	TPM1	Isoform 4 of Tropomyosin alpha-1 chain	0.313	0.616	0.894	1.78E-03	4
P55786	NPEPPS	Puromycin-sensitive aminopeptidase	0.109	0.281	0.553	2.08E-04	4
P55786–2	NPEPPS	Isoform 2 of Puromycin-sensitive aminopeptidase	0.107	0.278	0.557	2.16E-04	4
A2A274	ACO2	Aconitate hydratase, mitochondrial	0.021	0.497	1.364	2.79E-03	4
P13929	ENO3	Beta-enolase	0.173	0.641	0.974	2.43E-03	4
P09104	ENO2	Gamma-enolase	0.111	0.300	0.502	6.15E-04	4
P17174	GOT1	Aspartate aminotransferase, cytoplasmic	−0.012	0.559	1.330	5.12E-04	4
P02545	LMNA	Prelamin-A/C	0.096	0.254	0.410	3.43E-02	4
P62258	YWHAE	14–3-3 protein epsilon	0.183	0.504	0.751	5.12E-04	4
P61981	YWHAG	14–3-3 protein gamma	0.161	0.455	0.722	2.16E-04	4
P40925–3	MDH1	Isoform 3 of Malate dehydrogenase, cytoplasmic	0.101	1.045	1.823	1.14E-04	4
P78417	GSTO1	Glutathione S-transferase omega-1	0.071	0.276	0.510	1.09E-02	4
P20810–6	CAST	Isoform 6 of Calpastatin	0.123	0.401	0.550	3.24E-03	4
P09622	DLD	Dihydrolipoyl dehydrogenase, mitochondrial	0.108	0.552	0.919	7.57E-03	4
P42765	ACAA2	3-ketoacyl-CoA thiolase, mitochondrial	0.062	0.517	0.938	2.88E-02	4
P18669	PGAM1	Phosphoglycerate mutase 1	0.162	0.710	1.002	1.27E-03	4
P17540	CKMT2	Creatine kinase S-type, mitochondrial	0.366	1.105	1.568	1.11E-04	4
Q16881–5	TXNRD1	Isoform 5 of Thioredoxin reductase 1, cytoplasmic	0.039	0.163	0.280	1.33E-02	4
Q16881–3	TXNRD1	Isoform 3 of Thioredoxin reductase 1, cytoplasmic	0.039	0.164	0.278	1.20E-02	4
P99999	CYCS	Cytochrome c	0.058	0.964	1.780	2.16E-04	4
Q15124	PGM5	Phosphoglucomutase-like protein 5	0.251	0.908	1.369	1.11E-04	4
P31153	MAT2A	S-adenosylmethionine synthase isoform type-2	0.055	0.188	0.460	3.64E-02	4
P11766	ADH5	Alcohol dehydrogenase class-3	0.080	0.666	1.127	2.08E-04	4
P25786–2	PSMA1	Isoform Long of Proteasome subunit alpha type-1	0.056	0.260	0.450	3.91E-02	4
P16083	NQO2	Ribosyldihydronicotinamide dehydrogenase [quinone]	0.051	0.229	0.459	3.35E-02	4
O14818	PSMA7	Proteasome subunit alpha type-7	0.105	0.197	0.400	3.19E-02	4
P21266	GSTM3	Glutathione S-transferase Mu 3	0.120	0.355	0.617	3.32E-04	4
P28161	GSTM2	Glutathione S-transferase Mu 2	0.084	0.419	0.734	4.47E-03	4
E9PHN7	GSTM2	Glutathione S-transferase Mu 2	0.094	0.404	0.736	5.74E-03	4
P09488	GSTM1	Glutathione S-transferase Mu 1	0.126	0.335	0.679	1.01E-02	4
Q03013	GSTM4	Glutathione S-transferase Mu 4	0.112	0.328	0.668	1.06E-02	4
Q96CN7	ISOC1	Isochorismatase domain-containing protein 1	0.026	0.250	0.717	8.16E-03	4
Q9NQW7–3	XPNPEP1	Isoform 3 of Xaa-Pro aminopeptidase 1	0.042	0.166	0.390	3.62E-03	4
P49721	PSMB2	Proteasome subunit beta type-2	0.070	0.263	0.403	2.43E-02	4
P46940	IQGAP1	Ras GTPase-activating-like protein IQGAP1	0.068	0.048	0.323	3.37E-02	4
P25789	PSMA4	Proteasome subunit alpha type-4	0.084	0.265	0.508	3.49E-02	4
H0YLC2	PSMA4	Proteasome subunit alpha type	0.080	0.270	0.505	4.04E-02	4
P62140	PPP1CB	Serine/threonine-protein phosphatase PP1-beta catalytic subunit	0.096	0.227	0.335	3.31E-03	4
P62136	PPP1CA	Serine/threonine-protein phosphatase PP1-alpha catalytic subunit	0.089	0.188	0.311	1.12E-02	4
P36873–2	PPP1CC	Isoform Gamma-2 of Serine/threonine-protein phosphatase PP1-gamma catalytic subunit	0.085	0.204	0.310	8.50E-03	4
P55809	OXCT1	Succinyl-CoA:3-ketoacid coenzyme A transferase 1, mitochondrial	0.023	0.106	0.812	2.61E-03	4
P09417	QDPR	Dihydropteridine reductase	0.040	0.311	0.631	1.57E-02	4
Q9ULA0	DNPEP	Aspartyl aminopeptidase	0.072	0.308	0.562	3.17E-04	4
E7ETB3	DNPEP	Aspartyl aminopeptidase	0.066	0.311	0.577	3.89E-04	4
P28074	PSMB5	Proteasome subunit beta type-5	−0.031	0.157	0.372	4.54E-02	4
Q9NZL9	MAT2B	Methionine adenosyltransferase 2 subunit beta	0.067	0.114	0.386	2.88E-02	4
P41250	GARS	Glycine–tRNA ligase	0.053	0.179	0.302	2.49E-02	4
P55083–2	MFAP4	Isoform 2 of Microfibril-associated glycoprotein 4	0.111	0.215	0.350	1.56E-02	4
Q5JSH3	WDR44	WD repeat-containing protein 44	0.062	0.151	0.284	3.70E-02	4
Q8NCW5	APOA1BP	NAD(P)H-hydrate epimerase	0.044	0.290	0.642	1.56E-03	4
Q9Y3B8–3	REXO2	Isoform 3 of Oligoribonuclease, mitochondrial	0.046	0.700	0.940	2.42E-03	4
P30046	DDT	D-dopachrome decarboxylase	0.074	0.426	0.695	4.26E-02	4
Q8IW45	CARKD	ATP-dependent (S)-NAD(P)H-hydrate dehydratase	0.030	0.340	0.645	3.78E-02	4
P53041	PPP5C	Serine/threonine-protein phosphatase 5	0.116	0.323	0.673	1.97E-03	4
P26022	PTX3	Pentraxin-related protein PTX3	0.122	0.501	0.762	4.79E-04	4

TABLE I—*continued*

Uniprot accession number	Gene symbol	Protein name	Log2 iTRAQ ratio (average of 4 PMI patients)			Moderated F-test *p* value[a]	Cluster[b]
			10min vs. BL	1hr vs. BL	4hr vs. BL		
P34949	MPI	Mannose-6-phosphate isomerase	0.188	0.345	0.662	5.52E-04	4
Q06124	PTPN11	Tyrosine-protein phosphatase non-receptor type 11	−0.047	0.143	0.297	3.00E-02	4
Q96HC4–6	PDLIM5	Isoform 6 of PDZ and LIM domain protein 5	0.090	0.340	0.518	2.65E-02	4
Q96HC4	PDLIM5	PDZ and LIM domain protein 5	0.116	0.245	0.419	4.08E-02	4
O75390	CS	Citrate synthase, mitochondrial	0.004	0.325	1.456	5.12E-04	4
P61457	PCBD1	Pterin-4-alpha-carbinolamine dehydratase	0.156	0.408	1.044	1.71E-02	4
P28070	PSMB4	Proteasome subunit beta type-4	0.138	0.213	0.364	6.68E-03	4
J3QL71	SCRN2	Secernin-2	0.036	0.146	0.327	1.66E-02	4
O95817	BAG3	BAG family molecular chaperone regulator 3	0.118	0.346	0.513	1.45E-02	4
P45379	TNNT2	Troponin T, cardiac muscle	−0.067	0.432	1.743	5.07E-03	4
K7ER74	APOC4-APOC2	Protein APOC4-APOC2	−0.879	−0.574	0.495	1.56E-03	4
P55056	APOC4	Apolipoprotein C-IV	−0.517	−0.231	0.336	4.73E-02	4
P61601	NCALD	Neurocalcin-delta	0.028	0.181	0.241	3.17E-02	4
P63316	TNNC1	Troponin C, slow skeletal and cardiac muscles	0.320	0.370	1.313	2.19E-03	4
Q6ICJ4	Em:AP000351.3	Em:AP000351.3 protein	−0.062	0.398	0.893	4.61E-02	4
O75367	H2AFY	Core histone macro-H2A.1	0.220	0.354	0.711	3.44E-02	4
O75112	LDB3	LIM domain-binding protein 3	0.035	0.269	0.616	1.94E-02	4
Q96GD0	PDXP	Pyridoxal phosphate phosphatase	0.144	0.171	0.363	2.81E-02	4
Q99598	TSNAX	Translin-associated protein X	0.129	0.200	0.362	4.27E-02	4
P46976	GYG1	Glycogenin-1	−0.036	0.440	0.724	2.42E-02	4
Q8WZA9	IRGQ	Immunity-related GTPase family Q protein	0.101	0.187	0.540	3.00E-02	4
P49748–3	ACADVL	Isoform 3 of Very long-chain specific acyl-CoA dehydrogenase, mitochondrial	−0.156	0.874	2.159	1.69E-02	4
Q14896	MYBPC3	Myosin-binding protein C, cardiac-type	−0.092	0.140	0.719	4.59E-02	4
P38646	HSPA9	Stress-70 protein, mitochondrial	0.109	0.507	0.821	6.15E-04	4
P19429	TNNI3	Troponin I, cardiac muscle	−0.189	0.265	1.725	2.19E-02	4
P22888	LHCGR	Lutropin-choriogonadotropic hormone receptor	0.077	0.642	1.124	1.21E-02	4
Q5TZA2	CROCC	Rootletin	−0.022	0.159	0.623	1.67E-02	4
Q5TZA2–2	CROCC	Isoform 2 of Rootletin	−0.048	0.170	0.634	1.12E-02	4
Q13356–2	PPIL2	Isoform 2 of Peptidyl-prolyl cis-trans isomerase-like 2	0.037	0.114	0.556	3.72E-02	4
Q9H7B2	RPF2	Ribosome production factor 2 homolog	0.500	0.247	1.091	3.19E-02	4
Q07954	LRP1	Prolow-density lipoprotein receptor-related protein 1	−0.120	−0.155	−0.161	3.00E-02	5
P04114	APOB	Apolipoprotein B-100	−0.537	−0.583	−0.071	2.35E-02	5
P01009	SERPINA1	Alpha-1-antitrypsin	−0.583	−0.591	−0.193	4.61E-02	5
P49747	COMP	Cartilage oligomeric matrix protein	−0.084	−0.101	−0.181	4.57E-02	5
P03952	KLKB1	Plasma kallikrein	−0.555	−0.618	−0.660	3.29E-02	5
P01871	IGHM	Ig mu chain C region	−0.185	−0.195	−0.062	2.34E-02	5
P04220		Ig mu heavy chain disease protein	−0.181	−0.177	−0.059	1.72E-02	5
Q12805	EFEMP1	EGF-containing fibulin-like extracellular matrix protein 1	−0.410	−0.393	−0.457	1.39E-02	5
Q12805–5	EFEMP1	Isoform 5 of EGF-containing fibulin-like extracellular matrix protein 1	−0.416	−0.415	−0.460	1.63E-02	5
O75197	LRP5	Low-density lipoprotein receptor-related protein 5	−0.157	−0.231	−0.204	3.91E-02	5
P04083	ANXA1	Annexin A1	−0.349	−0.348	−0.335	1.11E-03	5
Q86U17	SERPINA11	Serpin A11	−0.215	−0.160	−0.350	2.28E-02	5
P18428	LBP	Lipopolysaccharide-binding protein	−0.348	−0.504	−0.476	3.13E-02	5
Q96CX2	KCTD12	BTB/POZ domain-containing protein KCTD12	−0.076	−0.116	−0.274	3.18E-02	5
Q9BXD5	NPL	N-acetylneuraminate lyase	−0.144	−0.286	−0.279	1.37E-02	5
Q6V0I7	FAT4	Protocadherin Fat 4	−0.106	−0.231	−0.236	4.32E-02	5
P14222	PRF1	Perforin-1	−0.130	−0.182	−0.248	1.88E-03	5
O15240	VGF	Neurosecretory protein VGF	−0.119	−0.325	−0.174	4.45E-02	5
Q96MU8–2	KREMEN1	Isoform 2 of Kremen protein 1	−0.209	−0.246	−0.193	7.30E-03	5
P09525	ANXA4	Annexin A4	−0.330	−0.442	−0.094	1.02E-02	5
P08236	GUSB	Beta-glucuronidase	−0.421	−0.437	−0.199	1.86E-02	5
B0YIW2	APOC3	Apolipoprotein C-III	−1.089	−1.115	−0.405	1.74E-02	5
Q5SPY9	NPDC1	Neural proliferation differentiation and control protein 1	−0.111	−0.263	−0.298	5.67E-03	5
P04211		Ig lambda chain V region 4A	−1.026	−0.813	−0.730	1.71E-02	5
Q92794	KAT6A	Histone acetyltransferase KAT6A	−0.490	−0.595	−0.047	3.68E-02	5
Q8N201	INTS1	Integrator complex subunit 1	−0.254	−0.328	−0.314	1.02E-02	5
Q2WGJ9	FER1L6	Fer-1-like protein 6	−0.474	−0.314	−0.124	2.65E-02	5
P54707–2	ATP12A	Isoform 2 of Potassium-transporting ATPase alpha chain 2	−0.253	−0.424	−0.252	8.50E-03	5
Q5VT52	RPRD2	Regulation of nuclear pre-mRNA domain-containing protein 2	−0.430	−0.601	−0.434	1.76E-03	5
Q9UNN5	FAF1	FAS-associated factor 1	−0.882	−0.640	−0.230	1.21E-02	5
Q8TE49–2	OTUD7A	Isoform 2 of OTU domain-containing protein 7A	−1.744	−1.530	−1.217	3.78E-03	5
O15072	ADAMTS3	A disintegrin and metalloproteinase with thrombospondin motifs 3	−0.110	−0.098	−0.487	2.04E-02	5

TABLE I—*continued*

Uniprot accession number	Gene symbol	Protein name	Log2 iTRAQ ratio (average of 4 PMI patients)			Moderated F-test *p* value[a]	Cluster[b]
			10min vs. BL	1hr vs. BL	4hr vs. BL		
Q6B0I6	KDM4D	Lysine-specific demethylase 4D	−1.120	−0.693	−0.551	4.60E-02	5
Q9NUL3	STAU2	Double-stranded RNA-binding protein Staufen homolog 2	−0.232	−0.548	−0.574	2.08E-02	5
J3KPX5	DNA2	DNA replication ATP-dependent helicase/nuclease DNA2	−0.266	−0.167	−0.109	4.91E-02	5
Q6P2E9	EDC4	Enhancer of mRNA-decapping protein 4	−0.318	−0.410	−0.065	3.64E-02	5
Q15761	NPY5R	Neuropeptide Y receptor type 5	−0.191	−0.544	−0.531	4.66E-02	5
Q9Y6Y0	IVNS1ABP	Influenza virus NS1A-binding protein	−0.116	−0.356	−0.104	4.48E-02	5
P09493–6	TPM1	Isoform 6 of Tropomyosin alpha-1 chain	0.335	0.635	0.906	6.15E-04	NA
E7EVY3	CAST	Calpastatin	0.129	0.405	0.536	4.11E-03	NA
Q99983	OMD	Osteomodulin	0.067	0.139	0.196	1.15E-02	NA
Q9Y5Z4	HEBP2	Heme-binding protein 2	0.110	0.481	0.277	4.26E-02	NA
P49354	FNTA	Protein farnesyltransferase/geranylgeranyltransferase type-1 subunit alpha	0.044	0.255	0.330	2.71E-02	NA
P31040	SDHA	Succinate dehydrogenase [ubiquinone] flavoprotein subunit, mitochondrial	0.093	1.056	1.311	9.41E-03	NA
P61224	RAP1B	Ras-related protein Rap-1b	0.294	0.361	0.363	2.96E-02	NA
P14174	MIF	Macrophage migration inhibitory factor	0.265	0.779	0.499	3.94E-03	NA
Q15843	NEDD8	NEDD8	0.039	0.200	0.258	2.79E-03	NA
O94913	PCF11	Pre-mRNA cleavage complex 2 protein Pcf11	0.209	0.141	0.210	2.61E-03	NA

[a] Benjamini-Hochberg corrected *p values are reported.*

[b] 323 out of 333 regulated proteins were clustered into 5 distinct clusters using Fuzzy C-means clustering. Proteins were assigned into clusters using membership value of > 0.7. Proteins with a membership value in between 0.5 and 0.7 weren't assigned to any cluster and marked as NA.

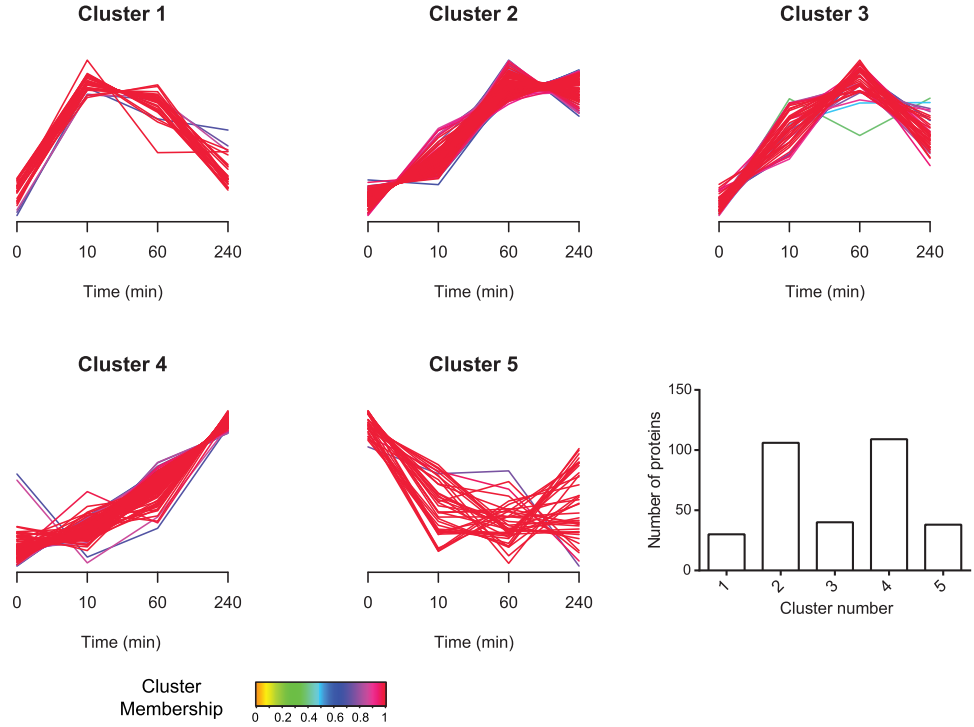

FIG. 4. **Cluster analysis of 333 regulated proteins.** 323 out of the 333 regulated proteins (p-Value < 0.05) in iTRAQ discovery study are grouped in 5 distinct clusters using fuzzy C-means clustering (13). Each line represents temporal behavior of a protein over the time course. X-axis represents the time points (baseline, 10 min, 1 h, and 4 h), and Y-axis represents normalized protein abundance. Proteins were assigned to a cluster based on the membership value of > 0.7. Proteins with membership value in between 0.5 and 0.7 were not assigned to any cluster. Bar graph on the lower right corner shows the number of proteins in each cluster.

indicate that even ten-plex analyses can be leveraged for higher throughput for biomarker discovery studies in plasma without significant loss in sensitivity. Furthermore, results from spiked in heavy labeled synthetic peptides indicate that ratio compression of TMT is similar to that of iTRAQ (supplemental Fig. S7).

iTRAQ-based Quantification of Proteins Correlates Well With MRM-MS Results—We developed a 23-plex immunoMRM

TABLE II
List of proteins and peptides in the 23-plex immunoMRM assay

Gene name	Protein name	Peptides
TNNI3	Troponin I	NITEIADLTQK
IL 33	Interleukin-33	TDPGVFIGVK
		VLLSYYESQHPSNESGDGVDGK
ACLP	Aortic carboxypeptidase-like protein 1	ILNPGEYR
		DTPVLSELPEPVVAR
FHL1	Four and a half LIM domains 1 isoform 5	AIVAGDQNVEYK
		NPITGFGK
MYL3	Myosin light chain 3	AAPAPAPPPEPERPK
		ALGQNPTQAEVLR
		HVLATLGER
TPM1	Isoform 4 of Tropomyosin alpha-1 chain	SIDDLEDELYAQK
		LVIIESDLER
		HIAEDADR
ITGB1	Isoform Beta-1C of Integrin beta-1	GEVFNELVGK
TAGLN2	Transgelin-2	ENFQNWLK
TAGLN1	Transgelin-1	AAEDYGVIK
FGL2	Fibroleukin	ELESEVNK
		EEINVLHGR
SCUBE2	Signal peptide, CUB and EGF-like domain-containing protein 2	GSVACECRPGFELAK
FSTL1	Follistatin-related protein 1	IQVDYDGHCK
		LDSSEFLK
SPON1	Spondin-1	VEGDPDFYKPGTSYR
		AQWPAWQPLNVR

(iMRM) assay (see "Methods") to quantify both known biomarkers of cardiac disease such as TNNI3 and novel candidate proteins that were prioritized for verification based on results from our earlier study (4) (Table II). Although most of these novel candidate proteins were in the up-regulated list from the current iTRAQ-based discovery study, some did not appear to be regulated based on iTRAQ quantification. To verify the discovery results and determine the correlation of iTRAQ quantification with a "gold standard" targeted approach, we applied the iMRM assay to 12 plasma samples from three patient time series experiments used in iTRAQ discovery. Each of the baseline, 10min, 1 h, and 4 h time point samples was analyzed in full process triplicate for all three patients (*i.e.* 36 samples, total). Fig. 5 shows the temporal trends observed in iTRAQ and iMRM experiments for selected proteins. The observed trends in abundance over the time course are the same by both quantification strategies for all three patients analyzed, although, as expected, the measured ratios are compressed in iTRAQ relative to iMRM. For example, levels for ACLP1 rise sharply at the 10min time point and decline thereafter with both the iTRAQ and iMRM workflows (Fig. 5*A*) whereas levels of FHL1 protein increase steadily to the 1 h time point and despite some decline remain elevated above baseline at the 4 h time point (Fig. 5*B*). FSTL1 (Fig. 5*C*) is an example of a protein thought to be regulated based on our earlier label free discovery experiments, but appears to be invariant over time after injury based on both iTRAQ and iMRM. supplemental Table S8 shows iMRM results for all of the proteins across the three patients analyzed.

DISCUSSION

Biomarker discovery approaches using MS-based proteomics have suffered from a lack of throughput, detection sensitivity, and quantitative precision that contributes to both false positive and false negative results. Particularly in plasma proteomics, where the objective of deep profiling for candidate discovery is challenged by the dynamic range and complexity of the matrix, extensive sample fractionation has also increased noise and decreased throughput. We have developed a comprehensive workflow for discovery proteomics in plasma that leverages isobaric labeling strategies, intensive depletion of abundant plasma proteins, optimized fractionation methods, improved reversed-phase column characteristics, and latest generation MS instrumentation to address these collective shortcomings.

The ability to increase sample analysis throughput is critically important for biomarker discovery experiments. In even the most carefully designed experimental and sample-selection strategies, biological variability because of both human and disease heterogeneity introduces noise that has a deleterious impact on candidate discovery. This contributes to lists of differential proteins that do not generalize, hence biomarker candidates that cannot be verified. This is made worse by the mismatch between high data dimensionality and low sample number that is characteristic of most transcriptome- and proteome-scale experiments and increases rates of false positive discovery. These problems are most directly addressed by increasing the number of samples analyzed, a strategy impeded by limitations in cost and throughput. Rel-

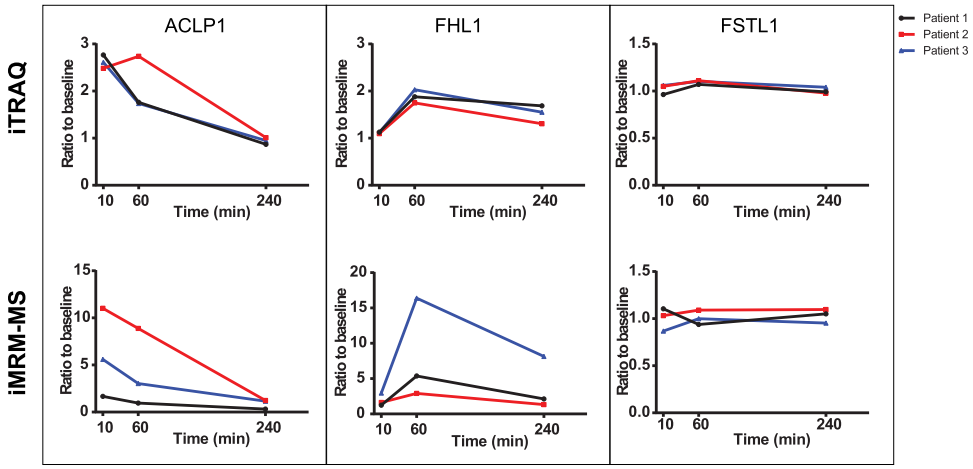

FIG. 5. **Correlation of iTRAQ discovery results with verification by iMRM.** Line plots show change over the time course for ACLP1 (A), FHL1 (B) and FSTL1 (C) as observed in iTRAQ discovery (top panel) and in iMRM verification (bottom panel) experiments for 3 out of the 4 PMI patients shown in black, red, and blue colors. For iTRAQ plots used normalized median protein ratio at 10min/BL, 1 h/BL and 4 h/BL for ACLP1, FHL1 and FSTL1. For iMRM plots ratios were obtained using peptide concentrations calculated for baseline, 10min, 1 h, and 4 h based on light to heavy peptide ratios observed for DTPVLSELPEPVVAR (ACLP1), AIVAGDQNVEYK (FHL1), and IQVDYDGHCK (FSTL1) peptides.

ative to transcriptional profiling, proteomics is further complicated by the need for sample enrichment and fractionation (often extensive) to enable sensitive detection of lower abundance proteins, which, in turn, further decreases throughput. The improvement in throughput we have achieved relative to "conventional" label-free approaches to deep discovery in plasma is dramatic. The six- to nine-fold improvement in throughput we have demonstrated using iTRAQ four-plex, while not a complete solution, represents substantial progress toward ameliorating the problem. In addition, our preliminary results using six-plex and ten-plex TMT reagents for labeling of plasma demonstrates that even further increases in analysis throughput are possible through higher multiplexing. These improvements in throughput derive from parallel downstream processing of a multiplexed samples, use of offline basic RP chromatography with concatenation of fractions prior to LC-MS/MS and use of nano-columns packed with sub-2 μm particle packing for online LC-MS/MS. Relative to our prior, label-free study (4), we estimate that 60% of the improvement in efficiency is because of the use of iTRAQ four-plex labeling which reduced on-instrument time by 75%. The remaining 40% of improvement derives from combined use of optimized off-line, basic reversed phase fractionation at high pH, optimized on-line nano-flow chromatography with heated columns packed with sub-2 μm packing, and much faster instrumentation (Q-Exactive). These factors together enabled reduction of the number of fractions requiring analysis from 80 to just 30. As a result, analyses that previously took one month with dedicated instrumentation are now being completed in 5 days using the four-plex reagent, and will be further reduced using the higher-plex reagents.

The chief cost drivers in most deep proteomics experiments employing fractionation prior to LC-MS/MS is instrument time and human labor for sample processing and data analysis. Although elements of our revised protocol (such as the use of isobaric labels and conversion to a tandem depletion strategy) add incremental cost to sample preparation, we estimate that total per-sample analysis cost was actually reduced by ~three-fold because of decreases in all four of the cost drivers identified above. Although label-free quantification methods continue to evolve and improve as a result of faster instrumentation and improved analysis algorithms (for example, see (30)), these experiments have higher cost because individual samples/fractions need to be analyzed in multiple replicate to ensure adequate statistical power. A disadvantage of the isobaric labeling approaches is that it is more difficult to derive a semi-quantitative estimate of absolute abundance in the sample. However, as the main objective of most proteomics discovery experiments is to assess relative changes in abundance across samples, we think that the positive attributes obtained with isobaric labeling outweigh this factor.

Increased throughput in proteomics experiments often comes at the cost of decreased sensitivity. However, as demonstrated, our approach couples substantial improvements in throughput with almost five-fold improvement in coverage of the plasma proteome compared with our prior workflow. The methods we used in our prior cardiovascular discovery (4), consistent with the state of the art at the time, yielded 900 or fewer confident protein identifications per sample (requiring two peptides/protein for identification). The iTRAQ four-plex workflow described here identified an average of 4641 proteins in each of 16 plasma samples with two or more distinct peptides per protein. Nearly 3400 proteins were detected and quantified in all patient samples. This comparison used the same type of samples collected by the same institutions using a similar experimental and sample processing paradigm, as

well as from head-to-head comparisons using a subset of identical samples.

Recently, Farrah and colleagues reported a set of 3553 high confidence plasma proteins (31) compiled after reanalysis of multiple high quality plasma proteomic datasets from multiple published sources using their centralized data processing workflow. In their analysis, 2568 of those 3553 proteins were detected by two or more peptide. We compared our list of 5304 proteins identified with two or more peptides with their list of proteins meeting the same criterion (supplemental Table S6, supplemental Fig. S1*C*). More than 85% of the proteins on their list were detected and quantified in our study. Moreover, half of the additional 982 proteins they included based on detection of only a single peptide were observed and quantified in our study by two or more peptides. Importantly, over half of the 5304 proteins confidently identified in our experiments are not included in the set published by Farrah and colleagues. Thus in four four-plex experiments we recapitulated and substantially surpassed the plasma proteomic characterization achieved by the union of multiple published plasma proteomes (31), or in any individual study published to date (for a recent review, see (32)). Proteins robustly identified in the Farrah dataset but not in ours included a few immunoglobulins and keratins that were either purposefully removed from our samples by immunoaffinity depletion or were not present in the database we used for searching.

Given the general perception that disease-specific markers, shed, secreted or leaked from affected tissue and massively diluted into the systemic circulation, are likely to be at low abundance in plasma (33), such increases in coverage seem very likely to be advantageous in biomarker discovery. Importantly, although in many discovery contexts the specific functional importance of improved depth of detection remains conjectural, here the proteins detected and quantified at the lower abundance levels include cardiac troponins I and T, established markers of myocardial injury of preeminent importance in the diagnosis and management of myocardial injury (34). Robust identification and measurement of these critical plasma biomarkers was barely evident in our earlier analyses; the new data provides a concrete demonstration of the utility of deep coverage.

Multiple components of our revised workflow contribute to improved detection and quantification of low abundance plasma proteins. For example, troponins were not identified until a second stage of depletion using Supermix was employed. The impact of tandem depletion was readily apparent in our global proteomic results. Total proteins we identified and quantified across three out of four iTRAQ experiments using IgY14/Supermix depletion represent a two-fold increase over the number of proteins quantified with a workflow identical except for use of IgY14 depletion alone. This augmentation of protein coverage by Supermix depletion exceeds that reported in the literature (21), likely because of the advantages of faster instrumentation and a globally more sensitive workflow. Analyzing the "depletate" from both depletion methods, although not currently practical given the added cost and time, is likely to further increase the number of proteins detected.

The present study also resulted in the identification of 333 regulated proteins across the four PMI patient samples. The majority of these candidate markers were elevated at 10 min post-ablation, and persisted for at least 60 min following injury. Sixty five percent of the candidates rise early and persist up to at least 4 h (clusters 2 and 4). This temporal profile is desirable for markers of myocardial injury. The new list of candidate biomarker proteins we identified to be regulated using iTRAQ includes 32 of the 52 proteins verified in our prior label-free study (4), as well as over 300 new candidates. Fifteen out of the remaining 20 proteins were detected and quantified in the current study, but were not observed to be regulated. Two of those proteins (FSTL1, SCUBE1) were analyzed by iMRM in the present study and shown to not be regulated, consistent with the iTRAQ results.

A central reason for our incorporation of isobaric labeling into the workflow was the potential to improve the precision of relative quantification in biomarker discovery relative to label-free approaches. Here we demonstrated that the reproducibility of quantification using iTRAQ, including all sources of variability introduced by the multidimensional sample processing strategy illustrated in Fig. 1, ranged from 16 to 24% (median CV). This level of reproducibility is only slightly lower than that routinely achieved in MRM-MS and iMRM-MS candidate biomarker verification studies (see (35, 36) and references therein). Although ultimately the most important measure of the utility of isobaric labeling will be demonstration of improved ability to identify functional biomarkers, a relevant surrogate is demonstration that results consistently reflect differential trends established by a "gold standard" quantification method. In MS-based proteomics, stable isotope dilution multiple reaction monitoring MS has emerged as the preferred method for targeted, quantitatively precise measurement of analytes in complex matrices (36). The 23 proteins quantified by iTRAQ in the context of the full discovery datasets exhibited good correlation with the iMRM-MS data that was obtained using stable isotope labeled peptides for quantification. Importantly, a subset of the proteins that we had observed to change in abundance in prior label-free experiments in a parallel set of patient samples were not observed to change using either iTRAQ or iMRM. These results further support that the quantitative precision obtainable using isobaric labeling in a discovery setting reflect real differences in the samples analyzed and form a more reliable basis on which to decide whether to configure more quantitative assays for, be they MS-based or Ab-based.

Compression of ratios is a well-known phenomenon with isobaric labeling (29, 37, 38). It is caused by co-isolation and fragmentation of iTRAQ-labeled peptide precursors, resulting in mass-tag ions from unrelated peptides merging and the

respective sources being indistinguishable. In the discovery experiments, the iTRAQ ratios for spiked heavy peptides were compressed up to two-fold in depleted plasma *versus* theoretical. Interestingly, the larger the actual fold difference the larger the extent of compression observed. This effect was also observed in the iMRM *versus* iTRAQ ratio comparisons where, for the most extreme case (Fig. 5, FHLI, patient 3), a ca. sixfold change in abundance measured by iMRM was observed as only a twofold change by iTRAQ. The smallest known differentials evaluated in the present study were two-fold differences for all of the 97 spiked heavy peptides. The median observed difference in the iTRAQ data for this set of peptides was 1.67, close to theoretical. Although false negatives could occur in isobaric labeling experiments, especially for proteins undergoing small changes in abundance, we have no evidence for them in the present study.

The results presented here provide clear demonstration of the value of using isobaric mass tag reagents in plasma-based biomarker discovery experiments to increase sample analysis throughput while providing very high sensitivity of analysis, and to derive high confidence lists of regulated proteins. We have leveraged human "perturbational" experiments in which each person serves as their own biologic control across a series of time points. This experimental paradigm enhances our statistical power to look for quantitative differences from baseline. We acknowledge, however, that observed differences between individuals (both biologic and technical) may also be considerable. Ultimately, any biomarker that emerges from our discovery work must then be tested across large heterogeneous groups of individuals (cases, controls, "at risk" individuals, etc.) using more high throughput methodologies.

The raw mass spectrometry data and the sequence database used for searches may be downloaded from MassIVE (http://massive.ucsd.edu) using the identifier: MSV000079033. Download this dataset directly from ftp://MSV000079033:a@massive.ucsd.edu.

Acknowledgments—We thank Dr. Robert Cole, Director of Mass Spectrometry and Proteomics Facility, Johns Hopkins School of Medicine for re-analysis of his iTRAQ proteomic data and for useful discussions.

* This work was supported in part by grants from National Institutes of Health: HHSN268201000033C and R01HL096738 from NHLBI (to REG and SAC) and Grants U24CA160034 from NCI Clinical Proteomics Tumor Analysis Consortium initiative and 5U01CA152990-05 from the NCI Early Detection Research Network program (to SAC).

S This article contains supplemental Figs. S1 to S7 and Tables S1 to S8.

¶ To whom correspondence should be addressed: Director of Proteomics, Broad Institute of MIT and Harvard, 7 Cambridge Center, Cambridge, MA 02142 Tel.: 617-714 7630; Fax: 617-714-8957; E-mail: scarr@broad.mit.edu; Tel: 617-714-7650; Email: hasmik@broadinstitute.org.

REFERENCES

1. Cao, Z. J., Tang, H. Y., Wang, H., Liu, Q., and Speicher, D. W. (2012) Systematic comparison of fractionation methods for in-depth analysis of plasma proteomes. *J. Proteome Res.* **11,** 3090–3100
2. Song, C. X., Ye, M. L., Han, G. H., Jiang, X. N., Wang, F. J., Yu, Z. Y., Chen, R., and Zou, H. F. (2010) Reversed-phase-reversed-phase liquid chromatography approach with high orthogonality for multidimensional separation of phosphopeptides. *Anal. Chem.* **82,** 53–56
3. Wang, Y. X., Yang, F., Gritsenko, M. A., Wang, Y. C., Clauss, T., Liu, T., Shen, Y. F., Monroe, M. E., Lopez-Ferrer, D., Reno, T., Moore, R. J., Klemke, R. L., Camp, D. G., and Smith, R. D. (2011) Reversed-phase chromatography with multiple fraction concatenation strategy for proteome profiling of human MCF10A cells. *Proteomics* **11,** 2019–2026
4. Addona, T. A., Shi, X., Keshishian, H., Mani, D. R., Burgess, M., Gillette, M. A., Clauser, K. R., Shen, D. X., Lewis, G. D., Farrell, L. A., Fifer, M. A., Sabatine, M. S., Gerszten, R. E., and Carr, S. A. (2011) A pipeline that integrates the discovery and verification of plasma protein biomarkers reveals candidate markers for cardiovascular disease. *Nat. Biotechnol.* **29,** 635-U119
5. Jones, K. A., Kim, P. D., Patel, B. B., Kelsen, S. G., Braverman, A., Swinton, D. J., Gafken, P. R., Jones, L. A., Lane, W. S., Neveu, J. M., Leung, H. C., Shaffer, S. A., Leszyk, J. D., Stanley, B. A., Fox, T. E., Stanley, A., Hall, M. J., Hampel, H., South, C. D., de la Chapelle, A., Burt, R. W., Jones, D. A., Kopelovich, L., and Yeung, A. T. (2013) Immunodepletion plasma proteomics by tripleTOF 5600 and Orbitrap elite/LTQ-Orbitrap Velos/Q exactive mass spectrometers. *J. Proteome Res.* **12,** 4351–4365
6. Cole, R. N., Ruczinski, I., Schulze, K., Christian, P., Herbrich, S., Wu, L., DeVine, L. R., O'Meally, R. N., Shrestha, S., Boronina, T. N., Yager, J. D., Groopman, J., and West, K. P. (2013) The plasma proteome identifies expected and novel proteins correlated with micronutrient status in undernourished Nepalese children. *J. Nutr.* **143,** 1540–1548
7. Pichler, P., Kocher, T., Holzmann, J., Mazanek, M., Taus, T., Ammerer, G., and Mechtler, K. (2010) Peptide labeling with isobaric tags yields higher identification rates using iTRAQ four-plex compared to TMT six-plex and iTRAQ 8-Plex on LTQ orbitrap. *Anal. Chem.* **82,** 6549–6558
8. Sinclair, J., and Timms, J. F. (2011) Quantitative profiling of serum samples using TMT protein labelling, fractionation and LC-MS/MS. *Methods* **54,** 361–369
9. Lewis, G. D., Wei, R., Liu, E., Yang, E., Shi, X., Martinovic, M., Farrell, L., Asnani, A., Cyrille, M., Ramanathan, A., Shaham, O., Berriz, G., Lowry, P. A., Palacios, I. F., Tasan, M., Roth, F. P., Min, J. Y., Baumgartner, C., Keshishian, H., Addona, T., Mootha, V. K., Rosenzweig, A., Carr, S. A., Fifer, M. A., Sabatine, M. S., and Gerszten, R. E. (2008) Metabolite profiling of blood from individuals undergoing planned myocardial infarction reveals early markers of myocardial injury. *J. Clin. Invest.* **118,** 3503–3512
10. (2011) R Development Core Team. *R: a language and environment for statistical computing*, R Foundation for Statistical Computing, Vienna, Austria
11. Smyth, G. K. (2004) Linear models and empirical bayes methods for assessing differential expression in microarray experiments. *Statistical applications in genetics and molecular biology* 3, Article3
12. Benjamini, Y., and Hochberg, Y. (1995) Controlling the false discovery rate: A practical and powerful approach to multiple testing. *J. Roy. Statist. Soc.* **57,** 289–300
13. Futschik, M. (2012) Mfuzz: Soft clustering of time series gene expression data. R package version 2.18.0. http://itb.biologie.hu-berlin.de/~futschik/software/R/Mfuzz/.
14. Fagbami, L., Kuhn, E., Abbatiello, S. E., and Carr, S. A. (2013) Automated plasma processing for quantitative, targeted LC/MS analysis of proteins. *Agilent Technologies, Inc.*
15. Kuhn, E., Whiteaker, J. R., Mani, D. R., Jackson, A. M., Zhao, L., Pope, M. E., Smith, D., Rivera, K. D., Anderson, N. L., Skates, S. J., Pearson, T. W., Paulovich, A. G., and Carr, S. A. (2012) Interlaboratory evaluation of automated, multiplexed peptide immunoaffinity enrichment coupled to multiple reaction monitoring mass spectrometry for quantifying proteins in plasma. *Mol. Cell. Proteomics* 11, M111 013854
16. MacLean, B., Tomazela, D. M., Shulman, N., Chambers, M., Finney, G. L., Frewen, B., Kern, R., Tabb, D. L., Liebler, D. C., and MacCoss, M. J. (2010) Skyline: an open source document editor for creating and analyzing targeted proteomics experiments. *Bioinformatics* **26,** 966–968

17. Echan, L. A., Tang, H. Y., Ali-Khan, N., Lee, K., and Speicher, D. W. (2005) Depletion of multiple high-abundance proteins improves protein profiling capacities of human serum and plasma. *Proteomics* **5,** 3292–3303
18. Liu, T., Qian, W. J., Mottaz, H. M., Gritsenko, M. A., Norbeck, A. D., Moore, R. J., Purvine, S. O., Camp, D. G., 2nd, and Smith, R. D. (2006) Evaluation of multiprotein immunoaffinity subtraction for plasma proteomics and candidate biomarker discovery using mass spectrometry. *Mol. Cell. Proteomics* 5, 2167–2174
19. Pieper, R., Su, Q., Gatlin, C. L., Huang, S. T., Anderson, N. L., and Steiner, S. (2003) Multi-component immunoaffinity subtraction chromatography: An innovative step towards a comprehensive survey of the human plasma proteome. *Proteomics* **3,** 422–432
20. Patel, B. B., Barrero, C. A., Braverman, A., Kim, P. D., Jones, K. A., Chen, D. E., Bowler, R. P., Merali, S., Kelsen, S. G., and Yeung, A. T. (2012) Assessment of two immunodepletion methods: Off-target effects and variations in immunodepletion efficiency may confound plasma proteomics. *J. Proteome Res.* **11,** 5947–5958
21. Qian, W. J., Kaleta, D. T., Petritis, B. O., Jiang, H. L., Liu, T., Zhang, X., Mottaz, H. M., Varnum, S. M., Camp, D. G., Huang, L., Fang, X. M., Zhang, W. W., and Smith, R. D. (2008) Enhanced detection of low abundance human plasma proteins using a tandem IgY12-SuperMix immunoaffinity separation strategy. *Mol. Cell. Proteomics* **7,** 1963–1973
22. Ross, P. L., Huang, Y. L. N., Marchese, J. N., Williamson, B., Parker, K., Hattan, S., Khainovski, N., Pillai, S., Dey, S., Daniels, S., Purkayastha, S., Juhasz, P., Martin, S., Bartlet-Jones, M., He, F., Jacobson, A., and Pappin, D. J. (2004) Multiplexed protein quantitation in Saccharomyces cerevisiae using amine-reactive isobaric tagging reagents. *Mol. Cell. Proteomics* **3,** 1154–1169
23. Li, Z., Adams, R. M., Chourey, K., Hurst, G. B., Hettich, R. L., and Pan, C. L. (2012) Systematic comparison of label-free, metabolic labeling, and isobaric chemical labeling for quantitative proteomics on LTQ orbitrap Velos. *J. Proteome Res.* **11,** 1582–1590
24. Usaite, R., Wohlschlegel, J., Venable, J. D., Park, S. K., Nielsen, J., Olsson, L., and Yates, J. R. (2008) Characterization of global yeast quantitative proteome data generated from the wild-type and glucose repression Saccharomyces cerevisiae strains: The comparison of two quantitative methods. *J. Proteome Res.* **7,** 266–275
25. Mertins, P., Qiao, J. W., Patel, J., Udeshi, N. D., Clauser, K. R., Mani, D. R., Burgess, M. W., Gillette, M. A., Jaffe, J. D., and Carr, S. A. (2013) Integrated proteomic analysis of post-translational modifications by serial enrichment. *Nat. Methods* **10,** 634–637
26. Mertins, P., Yang, F., Liu, T., Mani, D. R., Petyuk, V. A., Gillette, M. A., Clauser, K. R., Qiao, J. W., Gritsenko, M. A., Moore, R. J., Levine, D. A., Townsend, R., Erdmann-Gilmore, P., Snider, J. E., Davies, S. R., Ruggles, K. V., Fenyo, D., Kitchens, R. T., Li, S., Olvera, N., Dao, F., Rodriguez, H., Chan, D. W., Liebler, D., White, F., Rodland, K. D., Mills, G. B., Smith, R. D., Paulovich, A. G., Ellis, M., and Carr, S. A. (2014) Ischemia in tumors induces early and sustained phosphorylation changes in stress kinase pathways but does not affect global protein levels. *Mol. Cell. Proteomics* **13,** 1690–1704
27. O'Donoghue, M., de Lemos, J. A., Morrow, D. A., Murphy, S. A., Buros, J. L., Cannon, C. P., and Sabatine, M. S. (2006) Prognostic utility of heart-type fatty acid binding protein in patients with acute coronary syndromes. *Circulation* **114,** 550–557
28. Ow, S. Y., Salim, M., Noirel, J., Evans, C., Rehman, I., and Wright, P. C. (2009) iTRAQ underestimation in simple and complex mixtures: "the good, the bad and the ugly". *J. Proteome Res.* **8,** 5347–5355
29. Mertins, P., Udeshi, N. D., Clauser, K. R., Mani, D. R., Patel, J., Ong, S. E., Jaffe, J. D., and Carr, S. A. (2012) iTRAQ labeling is superior to mTRAQ for quantitative global proteomics and phosphoproteomics. *Mol. Cell. Proteomics* 11, M111 014423
30. Cox, J., Hein, M. Y., Luber, C. A., Paron, I., Nagaraj, N., and Mann, M. (2014) Accurate proteome-wide label-free quantification by delayed normalization and maximal peptide ratio extraction, termed MaxLFQ. *Mol. Cell. Proteomics* **13,** 2513–2526
31. Farrah, T., Deutsch, E. W., Omenn, G. S., Sun, Z., Watts, J. D., Yamamoto, T., Shteynberg, D., Harris, M. M., and Moritz, R. L. (2014) State of the human proteome in 2013 as viewed through PeptideAtlas: Comparing the kidney, urine, and plasma proteomes for the biology- and disease-driven human proteome project. *J. Proteome Res.* **13,** 60–75
32. Pernemalm, M., and Lehtio, J. (2014) Mass spectrometry-based plasma proteomics: state of the art and future outlook. *Expert Rev. Proteomic* **11,** 431–448
33. Rifai, N., Gillette, M. A., and Carr, S. A. (2006) Protein biomarker discovery and validation: the long and uncertain path to clinical utility. *Nat. Biotechnol.* **24,** 971–983
34. Antman, E. M., Tanasijevic, M. J., Thompson, B., Schactman, M., McCabe, C. H., Cannon, C. P., Fischer, G. A., Fung, A. Y., Thompson, C., Wybenga, D., and Braunwald, E. (1996) Cardiac-specific troponin I levels to predict the risk of mortality in patients with acute coronary syndromes. *N. Engl. J. Med.* **335,** 1342–1349
35. Carr, S. A., Abbatiello, S. E., Ackermann, B. L., Borchers, C., Domon, B., Deutsch, E. W., Grant, R. P., Hoofnagle, A. N., Huttenhain, R., Koomen, J. M., Liebler, D. C., Liu, T., MacLean, B., Mani, D., Mansfield, E., Neubert, H., Paulovich, A. G., Reiter, L., Vitek, O., Aebersold, R., Anderson, L., Bethem, R., Blonder, J., Boja, E., Botelho, J., Boyne, M., Bradshaw, R. A., Burlingame, A. L., Chan, D., Keshishian, H., Kuhn, E., Kinsinger, C., Lee, J. S. H., Lee, S. W., Moritz, R., Oses-Prieto, J., Rifai, N., Ritchie, J., Rodriguez, H., Srinivas, P. R., Townsend, R. R., Van Eyk, J., Whiteley, G., Wiita, A., and Weintraub, S. (2014) Targeted peptide measurements in biology and medicine: Best practices for mass spectrometry- based assay development using a fit- for- purpose approach. *Mol. Cell. Proteomics* **13,** 907–917
36. Gillette, M. A., and Carr, S. A. (2013) METHOD OF THE YEAR Quantitative analysis of peptides and proteins in biomedicine by targeted mass spectrometry. *Nat. Methods* **10,** 28–34
37. Karp, N. A., Huber, W., Sadowski, P. G., Charles, P. D., Hester, S. V., and Lilley, K. S. (2010) Addressing accuracy and precision issues in iTRAQ quantitation. *Mol. Cell. Proteomics* **9,** 1885–1897
38. Savitski, M. M., Mathieson, T., Zinn, N., Sweetman, G., Doce, C., Becher, I., Pachl, F., Kuster, B., and Bantscheff, M. (2013) Measuring and managing ratio compression for accurate iTRAQ/TMT quantification. *J. Proteome Res.* **12,** 3586–3598